Renormalisation in lattice QCD

Jon Ivar Skullerud

Doctor of Philosophy

The University of Edinburgh

1996

To my father

Abstract

This thesis investigates various aspects of the relation between the lattice and continuum formulations of quantum field theories, in particular QCD. The aim of this is to gain a better insight into the theory of QCD, and to be able to relate more accurately the numbers obtained from lattice simulations to experimental values for physical quantities.

The first part of this thesis (chapters 1 and 2) gives a general introduction to quantum field theory, with emphasis on the lattice formulation of QCD. The first chapter describes the functional integral formulation of gauge theories and how it can be used to study these theories non-perturbatively by discretising the space-time variables.

The second chapter discusses the principles behind the renormalisation of these theories. The Ward and Slavnov–Taylor identities that are preserved non-perturbatively, and can be invoked when renormalising the theory, are derived. The final part of this chapter discusses the renormalisation of composite operators, using both perturbative and non-perturbative methods. In particular, it is shown how the chiral Ward identities can be used to extract renormalisation constants for the axial and vector currents and the ratio of the scalar to the pseudoscalar density.

In chapter 3, results for Z_A, Z_V and Z_P/Z_S at $\beta = 6.2$ are presented and their effects on calculations of physical quantities like decay constants are dicussed.

The final chapter investigates the quark–gluon vertex. The form factors of the off-shell vertex function, and the symmetries and Slavnov–Taylor identities that may be used to reduce these form factors, are discussed. I then outline a method for extracting the running coupling from the vertex function. This also includes a discussion of the quark and gluon field renormalisation.

Details of computation and results for the vertex function in the Landau gauge

are then presented, and these results are compared with other determinations of the running coupling and with other more general studies of the vertex function.

Declaration

This thesis has been composed wholly by me and contains my own work, carried out as a member of the UKQCD collaboration. The work presented in chapter 4 was carried out initially in collaboration with David Henty and Claudio Parrinello.

Some of the material in chapter 3 has been presented in

- D.S. Henty, R.D. Kenway, B.J. Pendleton, J.I. Skullerud, *Phys. Rev.* **D51**, 5323 (1995)

A brief outline of the method employed in chapter 4 has been presented in

- J.I. Skullerud, *Nucl. Phys.* **B (Proc. Suppl.) 47**, 398 (1996)

jon ivar skullerud

Acknowledgements

This thesis would never have come into existence if my father had not persuaded me to devote my PhD to gaining experience and insight into 'normal' physics research, at a time when I was inclined towards dividing my efforts equally between physics, mathematics and philosophy. It is therefore dedicated to him. I am eternally grateful for the moral support I have received from him and from my mother throughout the 4 years I have spent on this work.

I wish to thank my supervisors Brian Pendleton and Richard Kenway for their guidance and encouragement during my time here. Special thanks go to David Henty, with whom I worked both on the main projects in this thesis, and who was always there to help when I got stuck. Special thanks also to Claudio Parrinello, who suggested and got me started on the project which now comprises chapter 4, and who has given valuable guidance up to the very end. I would also like to thank David Richards, who helped me when David and Claudio had left the department.

Thanks also to all those with whom I have shared offices, coffee breaks, problems and frustrations during my years in the department, giving my time within the walls of JCMB more than a bit of colour.

The financial support I received from the Norwegian Research Council the first three years has been sufficient to keep me going the full four years, and without that support this would never have seen the light of day.

Finally, to all my friends in the Green Society and Green Student Network, who have given me most of my life outside the department and a purpose beyond just finishing a PhD. My life would not have been a tenth as interesting without all the gatherings, actions, gardening and general social get-togethers with the rest of the 'greenies'. Thanks a lot to you all!

Contents

Chapter 1

Quantum field theory and lattice QCD

1.1 Basic philosophical idea

Quantum field theory claims to describe the basic constitution of the world, providing the principles underlying all matter and forces — the 'basic matter' and 'basic force'. Although its current incarnation, the Standard Model, is not a final theory (it must be supplemented with general relativity, for one thing), most improvements and suggestions for further developments of the Standard Model are formulated within the framework of quantum field theory. The entities it concerns itself with are remote from ordinary life — their typical scales are 15 levels of magnitude down, at the subatomic and subnuclear level, and most of them are only 'observed' in big, complex detectors in big accelerators. Much of lattice QCD concerns itself with bridging the first part of the gap with the macroscopic world – constructing hadrons and hadronic physics from the world of quark and gluon fields.

The essence of the world as described by quantum field theory has some notable features, distinguishing it from previous fundamental theories, which describe the world at more 'normal' scales.

Matter and force are treated on the same footing, so the 'basic matter' and the

'basic force' are much the same kind of entity. There is a rough identification of matter with fermions and of force with (gauge) bosons, but even that is no longer the case in supersymmetric theories.

The basic entities of the theory are fields, derived from a mathematical language originally used for describing and explaining forces. More precisely, the basic entities are operator fields, which create and destroy particle — 'matter' — states. This may be the first time in fundamental physics since Aristotle that forces have taken priority over matter.

Rather than individual particles, it is the species of particles that is considered primary, since each field corresponds to one particle species — undermining the individuality that has traditionally been seen as a defining property of matter.

The entities that are considered fundamental by the theory are not those that can be 'observed' by experiment. Since it is not possible to separate a particle or field from its interactions, the fields and parameters must be renormalised so that everything is described in terms of the 'observable' fields which are dressed with self-interactions. Much of this thesis concerns itself with this aspect of the theory.

1.2 Functional integral formalism

The dynamics of the fields (and the corresponding particles) are determined by the action S, which is a functional of the fields. The action must satisfy the conditions of locality, microcausality and Poincaré invariance. Specifically, the requirement of locality implies that the action can be written as an integral $S = \int d^4x \mathcal{L}(x)$ of the Lagrangian $\mathcal{L}$, which is a function of the fields and their derivatives.

There are two formalisms commonly used for quantising field theories. The canonical operator formalism treats the fields as operators which create and destroy particles, and imposes commutation relations between them, like the equal time

commutator between fields and canonical momenta, or Heisenberg's equation of motion. The functional integral formalism treats the fields as ordinary variables (or Grassmann variables in the case of fermionic fields) with a weight for each field configuration $[\Phi]$ given by $\exp(iS[\Phi])$. By integrating over all possible field configurations one can obtain the Green functions or vacuum expectation values of any product of field variables

$$\begin{aligned}\langle\Phi(x_1)\Phi(x_2)\cdots\Phi(x_n)\rangle &\equiv \langle 0|T(\Phi(x_1)\Phi(x_2)\cdots\Phi(x_n)|0\rangle \\ &= \int \mathcal{D}\Phi\Phi(x_1)\Phi(x_2)\cdots\Phi(x_n)e^{iS[\Phi]} \qquad (1.1)\end{aligned}$$

where Φ refers to any field — scalar, spinor, vector or tensor — and $x_1, x_2, \ldots$ are general coordinates, referring to both space–time and internal indices.

The Green functions contain all the physical information of the theory. In particular, they are related to transition amplitudes between external n-particle states through the Lehmann–Symanzik–Zimmermann reduction formula

$$\begin{aligned}&\langle p_1 p_2 \ldots p_n, \text{out}|q_1 q_2 \ldots q_m, \text{in}\rangle \\ &= (iZ_\Phi^{-1/2})^{n+m+1}\int d^4y_1\cdots d^4x_m \exp(\textstyle\sum ip_k y_k - \sum iq_k x_k) \\ &\times (\Box_{y_1}+m^2)\cdots(\Box_{x_m}+m^2)\langle\Phi(y_1)\cdots\Phi(x_m)\rangle \qquad (1.2) \\ &+ \quad \text{disconnected terms}\end{aligned}$$

For fermionic fields, $(\Box + m^2)$ is replaced by the fermion operator $(i\not{\partial} + m)$.

The Green functions can all be expressed in terms of the generating functional

$$Z[J] = \int \mathcal{D}\Phi e^{iS[\Phi]+i\int d^4x J(x)\cdot\Phi(x)} \qquad (1.3)$$

which gives

$$\mathcal{G}^{(1)}(x) \equiv \langle\Phi(x)\rangle = \frac{\delta}{i\delta J(x)}Z[J]\Big|_{J=0} \qquad (1.4)$$

$$\mathcal{G}^{(2)}(x_1, x_2) \equiv \langle \Phi(x_1)\Phi(x_2) \rangle \quad = \quad \frac{\delta}{i\delta J(x_1)} \frac{\delta}{i\delta J(x_2)} Z[J]\Big|_{J=0} \qquad (1.5)$$

etc.

We are normally interested only in the *connected* Green functions, which can be derived from the generating functional $W[J]$ where

$$Z[J] = e^{W[J]} \qquad (1.6)$$

The one-particle irreducible (proper) Green functions $\Gamma^{(n)}(x_1, \ldots, x_n)$ can be defined in terms of their corresponding Feynman diagrams: They are truncated (all external propagator legs are removed) and cannot be divided into subdiagrams by cutting one internal line. All Feynman diagrams and Green functions can be written in terms of proper functions. They can also be derived from the effective action $\Gamma[\Phi]$, which is arrived at by a Legendre transformation of $W[J]$

$$i\Gamma[\Phi] = W[J] - i \int d^4x J(x)\Phi(x) \qquad (1.7)$$

where

$$\Phi(x) \quad = \quad \frac{\delta}{i\delta J(x)} W[J] \qquad (1.8)$$

$$\Rightarrow J(x) \quad = \quad -\frac{\delta \Gamma}{\delta \Phi(x)} \qquad (1.9)$$

We then have

$$\Gamma^{(n)}(x_1, \ldots, x_n) = \frac{\delta}{\delta\Phi(x_1)} \cdots \frac{\delta}{\delta\Phi(x_n)} \Gamma[\Phi]\Big|_{\Phi=\Phi_c} \qquad (1.10)$$

where $\Phi_c = \langle \Phi \rangle$ are the classical fields. These proper functions are the building blocks of perturbation theory and the renormalisation programme.

1.3 Gauge theories

1.3.1 The gauge principle

In addition to the external space–time degrees of freedom (including Dirac and Lorentz indices for spinors and vectors/tensors), the matter fields have internal degrees of freedom, which can be expressed as one or more complex phases $\Phi = \Phi_0 e^{-igt^a\theta^a}$. The physics of the system should be independent of how these phases are chosen, so it should be invariant under local changes of phase, or local gauge transformations. This leads to the introduction of gauge fields A^a_μ and covariant derivatives $D_\mu = \partial_\mu + igt^a A^a_\mu$. The transformation of the matter fields

$$\Phi(x) \to e^{-igt^a\theta^a(x)}\Phi(x) \tag{1.11}$$

is compensated by the transformation of the gauge fields

$$A_\mu(x) \to e^{-igt^a\theta^a(x)}(A_\mu(x) - \frac{i}{g}\partial_\mu)e^{igt^a\theta^a(x)}, \tag{1.12}$$

where $A_\mu(x) = t^a A^a_\mu(x)$. Then the covariant derivative of the matter field will transform in the same way as the matter field itself:

$$D_\mu\Phi(x) \to e^{-igt^a\theta^a(x)}D_\mu\Phi(x) \tag{1.13}$$

Alternatively, this can be understood as parallel transport in a general coordinate space. In this picture, the matter fields are vectors (fibre bundles) in the curved space of gauge coordinates. The connection between two adjacent fibre bundles is provided by the gauge field A_μ — when a vector is parallel transported from x to $x + dx$, it picks up a phase $igA_\mu(x)dx_\mu$:

$$\Phi(x + dx) = \Phi(x) + igA_\mu(x)\Phi(x)dx_\mu \tag{1.14}$$

or, non-infinitesimally,

$$\Phi(x') = \mathcal{P} e^{ig \int_x^{x'} A_\mu(z) dz_\mu} \Phi(x) \tag{1.15}$$

where path-ordering $\mathcal{P}$ means that the later points in the path come to the left. In this picture, gauge invariance can be seen to be an expression of translation invariance in this space.

The dynamics of the gauge fields themselves is given by the Yang–Mills action

$$\mathcal{L}^{YM} = -\frac{1}{4} \mathrm{Tr} F_{\mu\nu} F^{\mu\nu} \tag{1.16}$$

where $F_{\mu\nu} = -\frac{i}{g}[D_\mu, D_\nu]$ is the field tensor (curvature tensor, in the geometric picture), which transforms as

$$F_{\mu\nu}(x) \to e^{-igt^a\theta^a(x)} F_{\mu\nu}(x) e^{igt^a\theta^a(x)}, \tag{1.17}$$

so $\mathcal{L}^{YM}$ is gauge invariant, as it should be.

1.3.2 Quantising gauge theories

The extra, unphysical gauge degrees of freedom lead to problems when one tries to quantise gauge theories, since the naive path integral will contain an infinite number of contributions from gauge equivalent configurations. This manifests itself in the propagator $D^{ab}_{\mu\nu}(x-y) = \langle A^a_\mu(x) A^b_\nu(y) \rangle$ being ill-defined, or its inverse $\Gamma^{AA}(x,y)$ singular.[1] To avoid this, we factor out the integration over the gauge

[1] This is only really a problem when one tries to perform a saddle point approximation to the functional integral, ie in perturbation theory. If we instead, as in lattice simulations, evaluate the functional integral directly, the problem does not arise.

group by inserting

$$1 = \Delta_{FP}[A_\mu(x)] \int \mathcal{D}g(x)\delta(F[A^g_\mu(x)]), \tag{1.18}$$

where F is a gauge non-invariant functional of A_μ, into the path integral. After reordering, the full partition function for a pure gauge theory becomes

$$Z = \int \mathcal{D}g \int \mathcal{D}A \Delta_{FP}[A]\delta(F[A])e^{iS[A]} \tag{1.19}$$

Both the gauge fixing term $\delta(F[A])$ and the Faddeev–Popov term $\Delta_{FP}[A]$ can be expressed as exponentials of a local action. In particular, for a covariant gauge, $F^a(x) = \partial^\mu A^a_\mu(x) - B^a(x)$, we can write

$$\int \mathcal{D}B(x) e^{-\frac{i}{2\xi}\int d^4x B^2(x)} \prod_{x,a} \delta(F^a(x)) = e^{-\frac{i}{2\xi}\int d^4x (\partial^\mu A^a_\mu(x))^2} \tag{1.20}$$

while

$$\Delta_{FP}[A] \equiv \det \frac{\delta F}{\delta \alpha} = \det \mathcal{M} = \int \mathcal{D}\overline{\eta}\mathcal{D}\eta e^{-i\int d^4x d^4y \overline{\eta}_a(y) \frac{\delta F^a(y)}{\delta \alpha_b(x)} \eta_b(x)} \tag{1.21}$$

where $\alpha^a(x)$ is the parameter for an infinitesimal gauge transformation, and $\overline{\eta}, \eta$ are scalar anticommuting variables or ghosts. For the covariant gauge, this can be rewritten

$$\begin{aligned} \delta F^a(x) &= \partial^\mu (\delta A_\mu)^a(x) = \partial^\mu D^{ab}_\mu \delta\alpha^b(x) \\ \Rightarrow \frac{\delta F^a}{\delta \alpha_b} &= \partial^\mu D^{ab}_\mu \end{aligned} \tag{1.22}$$

Including N_f flavours of fermion fields, the full Lagrangian for a gauge theory like QCD in a covariant gauge is

$$\mathcal{L}(x) = \mathcal{L}^{YM}(x) + \mathcal{L}^{F}(x) + \mathcal{L}^{GF}(x) + \mathcal{L}^{FP}(x) \tag{1.23}$$

where

$$\mathcal{L}^F(x) = \overline{\psi}(x)(i\not{D} - m)\psi(x) \tag{1.24}$$

$$\mathcal{L}^{GF}(x) = -\frac{1}{2\xi}(\partial^\mu A_\mu)^2 \tag{1.25}$$

$$\mathcal{L}^{FP}(x) = \partial_\mu \overline{\eta}(x) D^\mu \eta(x) \tag{1.26}$$

and $\mathcal{L}^{YM}$ is given by (1.16)

1.4 Euclidean quantum field theory

The functional integral in Minkowski space is not well-defined and is ill-suited for numerical studies. Therefore, most numerical studies, both those using Dyson–Schwinger equations and lattice simulations, are carried out in Euclidean space.

The Euclidean action and functional integral are obtained from the Minkowski space equivalents by the substitutions

$$\int d^4x \rightarrow -i \int d^4x^E \tag{1.27}$$

$$\gamma^\mu \partial_\mu \rightarrow i\gamma^E \cdot \partial^E \tag{1.28}$$

$$\gamma^\mu A_\mu \rightarrow -i\gamma^E \cdot A^E \tag{1.29}$$

$$A^\mu B_\mu \rightarrow -A^E \cdot B^E \tag{1.30}$$

where $a \cdot b = \sum_{i=1}^4 a_i b_i$, and the γ_μ^E's satisfy

$$\{\gamma_\mu^E, \gamma_\nu^E\} = 2\delta_{\mu\nu} \qquad \text{and} \qquad \gamma_5^E = -\gamma_1^E \gamma_2^E \gamma_3^E \gamma_4^E \tag{1.31}$$

Under this transformation, the proper Green functions are directly carried over to the Euclidean space, while the full, connected Green functions $G_C^{(n)}$ pick up a prefactor $i(-i)^n$.

This is equivalent to an analytic continuation (Wick rotation) $x^0 \rightarrow -ix_4$ of the

time variable in the complex plane. This continuation is valid provided the Green functions have no singularities in the third and first quadrant of the complex plane. This is usually true in perturbation theory, but not necessarily non-perturbatively. This problem may be overcome by *defining* the theory in Euclidean space and solving for the Euclidean position-space Green functions (Schwinger functions). These may then be continued back to Minkowski space – though quantities like masses and decay constants are invariant under the Wick rotation, so the analytic continuation to Minkowski space is not needed if this is all we are interested in.

A necessary condition for the Euclidean theory to be well-defined (or the analytic continuation to Minkowski space to be possible) is reflection positivity, which means that

$$\langle (\Theta F) F \rangle \geq 0 \tag{1.32}$$

where

$$\Theta F(\vec{x}, t) = \overline{F(\vec{x}, -t)} \tag{1.33}$$

for any functional F which depends only on the fields at positive times. This is specifically a statement about Schwinger functions, and is the Euclidean-space version of the spectral condition and requirement that the scalar product in Hilbert space is positive.

The Euclidean path integral is

$$Z = \int \mathcal{D}\Phi^E e^{-S^E[\Phi^E]} \tag{1.34}$$

where $S^E[\Phi^E]$ is arrived at using the transcription rules (1.27)–(1.31), and is real. The theory thus takes the form of a statistical mechanics problem, with a weight $e^{-S^E[\Phi]}$ given to each configuration $[\Phi]$, and lends itself to simulations using Monte Carlo methods. Hereafter, everything will be in Euclidean space unless explicitly stated otherwise, and the superscript ^{E} will be dropped.

1.5 Lattice QCD

In order to simulate the theory on a computer, with a finite number of variables, we discretise space–time to form a finite lattice, replacing $\int dx$ with $a\sum_x$ and derivatives with finite differences. The lattice fields $\Phi^L(x)$ are taken to be some average of the continuum fields over the space near x.

1.5.1 Lattice gauge fields

The gauge fields are represented by link fields $U_\mu(x)$ which belong to the gauge group G itself, rather than by the fields $A_\mu(x)$ which belong to the gauge algebra. The link fields are the parallel transporters

$$U(x, x+\hat{\mu}) = U_\mu(x) = e^{-igaA_\mu(x+\hat{\mu}/2)} \approx e^{ig\int_{x+\hat{\mu}}^{x} A_\mu(x)dx} \tag{1.35}$$

which transform a matter field at $x+\hat{\mu}$ to one at x, cf. section 1.3.1. Under a local gauge transformation $\Lambda(x)$ these will transform as

$$U_\mu^\Lambda(x) = \Lambda(x)U_\mu(x)\Lambda^{-1}(x+\hat{\mu}) \tag{1.36}$$

The continuum functional integral $\int \mathcal{D}A_\mu$ is replaced by

$$\int \mathcal{D}U = \prod_{x,\mu} \int dU_\mu(x) \equiv \prod_{\substack{\text{links} \\ b}} \int dU(b) \tag{1.37}$$

This is finite and well-defined for any compact group if for dU we use the invariant group measure (Haar measure), which obeys

$$\int_G f(U)dU = \int_G f(VU)dU = \int_G f(UV)dU \qquad \forall V \in G \tag{1.38}$$

$$\int_G dU = 1 \tag{1.39}$$

Since the functional integral is already well-defined, there is no need to fix the gauge if we want to compute gauge invariant quantities.

The gauge invariant quantities that can be constructed in this theory are

$$\Phi^\dagger(x)U(\mathcal{C}_{x,y})\Phi(y) \qquad \text{and} \qquad U(\mathcal{C}_{x,x})$$

where Φ is a matter (scalar or spinor) field which transforms as

$$\Phi^\Lambda = \Lambda\Phi \qquad\qquad (\Phi^\dagger)^\Lambda = \Phi^\dagger\Lambda^{-1} \tag{1.40}$$

and $U(\mathcal{C}_{x,y})$ is a parallel transporter $U(x,z_1)U(z_1,z_2)\cdots U(z_n,y)$ along any path $\mathcal{C} = (x, z_1, z_2, \ldots, z_n, y)$ joining x and y. The covariant forward derivative can be constructed as

$$D^L_\mu\Phi(x) = \frac{1}{a}[U_\mu(x)\Phi(x+\hat{\mu}) - \Phi(x)] \tag{1.41}$$

so that

$$\Phi^\dagger(x)D^L_\mu\Phi(x) = \frac{1}{a}[\Phi^\dagger(x)U_\mu(x)\Phi(x+\hat{\mu}) - \Phi^\dagger(x)\Phi(x)] \tag{1.42}$$

is obviously gauge invariant.

The pure gauge action is expressed in terms of closed loops, with the simplest being the Wilson action [1] (for a SU(N) gauge theory)

$$\begin{aligned} S_\square &= \frac{1}{g^2}\sum_x(12N - \Re\mathrm{e}\sum_{\mu<\nu}\mathrm{Tr}U^{\mu\nu}_\square(x)) \\ &\equiv \beta\sum_x\sum_{\mu<\nu}\left(1 - \frac{1}{N}\Re\mathrm{e}\mathrm{Tr}U^{\mu\nu}_\square(x)\right) \\ &= S^{YM} + \mathcal{O}(a^2) \end{aligned} \tag{1.43}$$

where $\beta = 2N/g^2$ and $U_{\square}^{\mu\nu}$ is the plaquette

$$U_{\square}^{\mu\nu}(x) \equiv U_\mu(x)U_\nu(x+\hat{\mu})U_\mu^\dagger(x+\hat{\nu})U_\nu^\dagger(x) \tag{1.44}$$

1.5.2 Lattice fermions

Fermions are represented on the lattice by anticommuting spinors ψ on the lattice sites. The fermion action can be discretised in a straightforward way:

$$\begin{aligned} S^F &= \sum_x \Big[\sum_\mu \left(\overline{\psi}(x)\gamma_\mu U_\mu(x)\psi(x+\hat{\mu}) - \overline{\psi}(x+\hat{\mu})U_\mu^\dagger(x)\gamma_\mu\psi(x) \right) \\ &\quad + m\overline{\psi}(x)\psi(x) \Big] \end{aligned} \tag{1.45}$$

This is called the *naive fermion action.* It suffers from the presence of *doublers* — unphysical zero modes of the fermion matrix. This can be seen from a simple inspection of the fermion matrix in momentum space:

$$M_{xy} = \sum_\mu \gamma_\mu(\delta_{y,x+\hat{\mu}} - \delta_{xy}) + m\delta_{xy} \tag{1.46}$$

$$M(p) = \sum_x e^{-ip(x-y)} M_{xy} = \sum_\mu \gamma_\mu \sin(p_\mu) + m \tag{1.47}$$

This is 0 for all $p_\mu \in \{0, \pi\}$. Since all zeros in the fermion matrix correspond to a particle (which can, in an interacting theory, be created in a pair production process), there will be not one, but 16 fermion species. Nielsen and Ninomiya [2] have shown that any lattice theory fulfilling the conditions of

- translational invariance
- locality
- hermiticity of the Hamiltonian

and with a set of locally defined, discretely valued conserved charges (fermion numbers) which are bilinear in the fermion fields will have an equal number of left- and right-handed particles for each set of quantum numbers. This means that neutrinos cannot be simulated on the lattice, and chiral symmetry cannot be preserved in lattice QCD.

Wilson [3] proposed a remedy for this problem by adding an extra irrelevant operator to the action

$$S^W = \frac{r}{a}\sum_x \left[\overline{\psi}(x)\psi(x) - \frac{1}{2}\sum_\mu \left(\overline{\psi}(x+\hat{\mu})U_\mu^\dagger(x)\psi(x) + \overline{\psi}(x)U_\mu(x)\psi(x+\hat{\mu})\right)\right] \tag{1.48}$$

which gives the doublers a mass on the scale of the cutoff a^{-1}. r is an arbitrary parameter, which is normally chosen to be equal to 1. This term explicitly breaks chiral symmetry.

The Wilson fermion action is often rewritten in terms of the hopping parameter κ as

$$\begin{aligned} S^{WF} &= \sum_x \Big\{\overline{\psi}(x)\psi(x) + \kappa\sum_\mu \overline{\psi}(x)[U_\mu(x)(\gamma_\mu - r)\psi(x+\hat{\mu}) \\ &\quad -U^\dagger(x-\hat{\mu})(\gamma_\mu + r)\psi(x-\hat{\mu})]\Big\} \end{aligned} \tag{1.49}$$

where

$$m = \frac{1-8\kappa r}{2\kappa} \tag{1.50}$$

This gives the momentum space free propagator

$$S(p) = \frac{-i\sum_\mu \gamma_\mu \sin(p_\mu a) + r\sum_\mu(1-\cos(p_\mu a)) + m}{\sum_\mu \sin^2(p_\mu a) + [r\sum_\mu(1-\cos(p_\mu a) + m]^2} \tag{1.51}$$

Since there is no chiral symmetry to prevent the fermions from acquring a dynamical mass, they will typically do so. This means that the massless limit can only be determined a posteriori as the value of κ where the pseudoscalar meson

is massless.

1.5.3 The quenched approximation

It is not possible to simulate Grassmann variables numerically in a direct way. But provided the action is bilinear in the fermion fields, they can be integrated out analytically. From the properties of Grassmann variables,

$$\int \psi d\psi = \frac{d}{d\psi}\psi = 1 \qquad \psi_i\psi_j = -\psi_j\psi_i \tag{1.52}$$

it follows that

$$\int \prod_i d\overline{\psi}_i d\psi_i e^{-\overline{\psi}_j M_{jk}\psi_k} = \det M \tag{1.53}$$

This means the effective gauge action is given by

$$\begin{aligned} Z &= \int \mathcal{D}U \det M[U] e^{-S_G[U]} = \int \mathcal{D}U e^{-S_G[U]+\ln\det M[U]} \\ &= \int \mathcal{D}U e^{-S_G^{eff}[U]} \end{aligned} \tag{1.54}$$

There exist several algorithms for simulating the fermion determinant, but these are computationally expensive, so most lattice simulations up to now have been performed in the *quenched approximation*, where one sets $\det M$=1. This is equivalent to ignoring the effect of fermions int the gauge distribution, ie ignoring vacuum polarisation effects from fermion loops. The quenched theory can be treated analytically as a theory with $N_f = 0$.

One would expect that setting $\det M$, which numerical simulations have shown to be a wildly fluctuating quantity, equal to 1, would be a very bad approximation. However, it turns out that most results obtained using this approximation agree quite well with experiment, suggesting that fermion loops only have marginal effects for most quantities.

1.6 Gauge fixing on the lattice

Although all physical quantities are gauge invariant and most of them can be computed on the lattice in a gauge invariant way, there are still many cases where gauge fixing is desirable or necessary. Most important among these are gauge dependent wave functions, and quark and gluon correlation functions (or anything involving matrix elements between quark and gluon states rather than hadronic states). The gauge can be fixed by applying a gauge transformation (1.36)on each link so that the resulting link variables conform to our gauge fixing prescription.

The most commonly used gauges in lattice studies are the Coulomb gauge $\nabla \cdot \vec{A} = 0$ and the Landau gauge $\partial_\mu A_\mu = 0$, corresponding to $\xi = 0$ in (1.25). The Landau gauge can be obtained by finding an extremal value for

$$F(\Lambda) = \|A^\Lambda\|^2 = \int \mathrm{Tr}(A^\Lambda_\mu(x) A^\Lambda_\mu(x)) d^4x \tag{1.55}$$

since, if we write $\Lambda(x) = \exp(it^a\theta^a(x))$, then

$$\frac{\delta F}{\delta \theta^a} = 0 \Rightarrow \partial_\mu A^a_\mu = 0 \tag{1.56}$$

This can be carried over to the lattice by replacing $\|A\|^2$ with

$$\|A\|^{2,LAT} = \sum_{x,\mu} \Re\mathrm{e}\mathrm{Tr} U_\mu(x) - 1 \tag{1.57}$$

However, this will not give a unique solution. Gribov [4] showed that in the continuum theory, there will be several non-trivial solutions satisfying this condition, with different $\Re\mathrm{e}\mathrm{Tr}U = F(\Lambda_{min})$, and this is also the case in the lattice theory [5]. The problem can be reduced, but not eliminated, by imposing additional conditions, eg. for the Faddeev–Popov matrix $|\mathcal{M}| > 0$.

More general gauges can be obtained by letting the gauge transformation be a

stochastic distribution rather than one definite transformation per gauge configuration. Specifically, the family of covariant gauges in (1.20) can be simulated by generating random matrices $B(x)$ with a distribution $\exp(-\frac{1}{2\xi}\mathrm{Tr}B(x))$ and fixing $\partial_\mu A_\mu(x) - B(x)$ in the same way as $\partial_\mu A_\mu(x)$ is fixed in the Landau gauge [6].

Another family of covariant gauges [7] is obtained by taking the gauge fixing functional

$$F[A] = e^{-S_{GF}} \qquad S_{GF} = \frac{\beta}{2}M^2 \int d^4x (A^a_\mu(x))^2 \tag{1.58}$$

to replace $\delta(F[A])$ in (1.18). This bypasses the problem of Gribov copies, and if $M \to \infty$, the point on the gauge orbit where $(A^a_\mu(x))^2$ reaches its global minimum is selected. This is equivalent to the Landau gauge $\partial_\mu A^a_\mu(x) = 0$, but with no copies. As $M \to 0$, the theory approaches a theory without gauge fixing.

This can be carried over to lattice simulations [8], replacing A^2 with $\Re\mathrm{e}\mathrm{Tr}U$, and evaluating the functional integral in two stages. For each configuration, a set of gauge transformations are generated with the weight $e^{-S_{GF}}$ and the (gauge dependent) operator we are interested in is averaged over those transformations, before the configuration average is taken.

It is also possible to transcribe the continuum gauge fixed action (1.23) to the lattice, and this is necessary when one wishes to perform perturbative lattice calculations. However, this does involve significant complications in computing the Faddeev–Popov determinant, and is not feasible for practical numerical simulations. Some numerical studies of ghost fields [9] have, however, been carried out.

1.7 Improved actions

Although all effects of discretisation should disappear as $a \to 0$, in any simulation using the Wilson actions (1.43) and (1.49) at realistic values of β, the $\mathcal{O}(a)$ and

$\mathcal{O}(a^2)$ discretisation errors may be significant. There are also lattice artefacts that are small at tree level, but may become large non-perturbatively, or at higher-loop order. Both these kinds of effects may give uncertainties of up to 20–30% in estimates of physical quantities, for the simulations that are possible today. It is therefore a great advantage if one can construct actions which reduce or avoid these problems.

1.7.1 Symanzik improvement

The idea of this programme [10] is to add higher-dimensional terms to the action to cancel order-by-order the discretisation effects. In the continuum (or, equivalently, on a much finer lattice), the lattice action, which is non-local, can be written as a local effective action

$$S = S_0 + aS_1 + a^2 S_2 + \ldots = \int d^4x [\mathcal{L}_0(x) + a\mathcal{L}_1(x) + \ldots] \tag{1.59}$$

Similarly, the renormalised composite lattice operator $\mathcal{O}_R$ can be represented by local effective fields

$$\mathcal{O}_R(x) = \mathcal{O}_0(x) + a\mathcal{O}_1(x) + a^2\mathcal{O}_2(x) + \ldots \tag{1.60}$$

where S_0 and $\mathcal{O}_0$ are the continuum action and operators respectively.

The operators that enter into $\mathcal{L}_1, \mathcal{O}_1$ etc can be constructed by considering their dimensionality and the symmetries they must obey, such as parity, charge conjugation, and Euclidean or lattice symmetries. In the improved action, counterterms with the same structure are added to cancel the contributions from $S_1, \mathcal{O}_1$ etc to the Green functions. Their coefficients can be computed perturbatively from the zero-momentum proper Green functions, or using a non-perturbative prescription [11].

Wilson's pure gauge action is already $\mathcal{O}(a)$-improved, while the Wilson fermion action has $\mathcal{O}(a)$ errors. We can write down the operators that enter into S_1^{WF}

$$\mathcal{O}^1 = \overline{\psi}\sigma_{\mu\nu}F_{\mu\nu}\psi \tag{1.61}$$

$$\mathcal{O}^2 = \overline{\psi}\overleftrightarrow{D}^2\psi \tag{1.62}$$

$$\mathcal{O}^3 = m\mathrm{Tr}F_{\mu\nu}F_{\mu\nu} \tag{1.63}$$

$$\mathcal{O}^4 = m(\overline{\psi}\not{D}\psi - \overline{\psi}\overleftarrow{\not{D}}\psi) \tag{1.64}$$

$$\mathcal{O}^5 = m^2\overline{\psi}\psi \tag{1.65}$$

Of these, $\mathcal{O}^2$ and $\mathcal{O}^4$ can be eliminated using the equations of motion (provided we are only considering on-shell quantities), while $\mathcal{O}^3$ and $\mathcal{O}^5$ imply a redefinition of the mass and coupling constant, respectively. So we are left with the Sheikholeslami–Wohlert [12] action

$$S^{SW} = S^{WF} + c_{SW}\int d^4x\overline{\psi}(x)\sigma_{\mu\nu}P_{\mu\nu}(x)\psi(x) \tag{1.66}$$

where $P_{\mu\nu}$ is some lattice representation of the field tensor $F_{\mu\nu}$. One possible choice, which makes the improved action depend only on nearest-neighbour couplings, is the cloverleaf term

$$P_{\mu\nu} = U_{\square}^{\mu\nu} - U_{\square}^{-\nu,-\mu} + U_{\square}^{\nu,-\mu} - U_{\square}^{\mu,-\nu} \tag{1.67}$$

The coefficient $c_{SW} = 1$ at tree level, but non-perturbative calculations [13] have shown it to be significantly different from this.

1.7.2 Tadpole improvement

Lattice operators, including those entering into the action, are usually constructed from or matched to continuum operators by expanding

$$U_\mu(x) = e^{iagA_\mu(x)} \to 1 + iagA_\mu(x) \tag{1.68}$$

However, the higher order terms in this expansion include 'tadpole diagrams' which generate power divergences in $1/a$, cancelling the powers of a in the expansion. This means that the vacuum expectation value of $U_\mu(x)$ (in some gauge) is smaller than 1 — the main contribution is from $-\langle A_\mu^2(x)\rangle < 0$ — and a better expansion would be

$$U_\mu(x) = u_0(1 + iagA_\mu(x)) \tag{1.69}$$

where u_0 represents the mean value of U_μ. Gauge invariance requires that u_0 is a constant. It can be defined in several ways, either as the expectation value of U_μ in the Landau (or some other) gauge, or by using the mean value of the plaquette,

$$u_0 = \left\langle \frac{1}{3}\mathrm{Tr}U_\square \right\rangle^{1/4}. \tag{1.70}$$

All these definitons give similar results [14].

The mean-field tadpole improvement prescription [14] simply replaces $U_\mu(x)$ with $U_\mu(x)/u_0$ everywhere in the action and in operators. For Wilson's gauge and fermion actions, this simply amounts to a rescaling of the parameters β and κ, but for improved actions, and when calculating certain matrix elements, it is non-trivial.

Chapter 2

Renormalisation

2.1 Symmetries and identities in QCD

It is a general feature of field theories that the existence of a continuous symmetry implies some identity for physical quantities. In classical field theories this manifests itself in Noether's theorem, linking every global, continuous symmetry with a conserved current. Thus, conservation of energy and momentum can be seen as a consequence of translational invariance, and electromagnetic current conservation a consequence of global gauge invariance.

In quantum field theory most of the interesting symmetries are expressed through Ward identities or Slavnov–Taylor identities between Green functions. The most important of these are derived from the gauge invariance of the theory.

2.1.1 The generic Ward identity

The generic Ward identity can be derived as a direct consequence of the invariance of Green functions under some local transformation. Consider a Green function

$$G(x_1, x_2, \ldots) = \langle \mathcal{O}(x_1, x_2, \ldots) \rangle = \int \mathcal{D}\Phi \mathcal{O}[\Phi](x_1, x_2, \ldots) e^{-S[\Phi]} \qquad (2.71)$$

If we postulate that G is invariant under some transformation of the fields, parametrised by a continuous variable $\omega(x)$, we have

$$0 = \frac{\delta G}{\delta \omega(x)} = \int \mathcal{D}\Phi \left(\frac{\delta \mathcal{O}}{\delta \omega(x)} - \mathcal{O} \frac{\delta S}{\delta \omega(x)} \right) e^{-S[\Phi]} \tag{2.72}$$

$$\Rightarrow \left\langle \frac{\delta \mathcal{O}}{\delta \omega(x)} \right\rangle - \left\langle \mathcal{O} \frac{\delta S}{\delta \omega(x)} \right\rangle = 0 \tag{2.73}$$

By choosing different operators $\mathcal{O}$ we can derive Ward identities connecting Green functions with any number of external legs and operator insertions. Alternatively, they can be expressed in a compact form as identities of the generating functionals.

2.1.2 Slavnov–Taylor identities

Consider the gauge fixed generating functional

$$e^{W[J]} = \int \mathcal{D}A \det \mathcal{M} e^{-\int d^4x (\mathcal{L}^{YM} + \frac{1}{2\xi} F^2 + J \cdot A)} \tag{2.74}$$

where F is the gauge fixing functional and $\det \mathcal{M}$ is the Faddeev–Popov determinant, cf. section 1.3.2. $\mathcal{D}A \det \mathcal{M}(A)$ is invariant under the gauge transformation $\delta A^a = D^{ab} \delta \alpha^b$, so we can transform the variables in the integral. This gives

$$e^{W[J]} = \int \mathcal{D}A \det \mathcal{M} e^{-\int d^4x (\mathcal{L}_{YM} + \frac{1}{2\xi} F^2 + J \cdot A + \frac{1}{\xi} F \mathcal{M} \delta\alpha + J \cdot D \delta\alpha)} \tag{2.75}$$

since $\delta F = \mathcal{M} \delta \alpha$.

Taking $\delta\alpha$ to be the nonlocal transformation $\delta\alpha = \mathcal{M}^{-1} \delta\omega$, and expanding to the lowest order in $\delta\omega$, we get

$$\int \mathcal{D}A \det \mathcal{M} \int d^4x \left(\frac{F}{\xi} + J \cdot D \mathcal{M}^{-1} \right) \delta\omega e^{-\int d^4x (\mathcal{L} + \frac{1}{2\xi} F^2 + J \cdot A)} = 0 \tag{2.76}$$

which implies

$$\frac{1}{\xi}F_a\left[\frac{\delta}{\delta J(x)}\right]e^{W[J]} = \int d^4y \left(J_a D_{bc}\left[\frac{\delta}{\delta J}\right]\right)(y)G_{ca}(y,x) \tag{2.77}$$

where

$$\mathcal{M}_{bc}\left[\frac{\delta}{\delta J(y)}\right]G_{ca}(y,x) = \delta_{ba}\delta^4(x-y)e^{W[J]} \tag{2.78}$$

This gives us the Slavnov–Taylor identities for full, connected Green functions. The identities for the proper functions can be obtained by observing that the action (with ghosts included) is invariant under the Becchi–Rouet–Stora transformation

$$\begin{aligned}
\delta A^\mu_a(x) &= D^\mu_{ab}(x)\eta_b(x)\delta\zeta \equiv sA\delta\zeta && (2.79)\\
\delta\overline{\eta_a}(x) &= \frac{1}{\xi}F_a[A(x)]\delta\zeta \equiv s\overline{\eta}\delta\zeta && (2.80)\\
\delta\eta_a(x) &= -\frac{g}{2}f_{abc}\eta_b(x)\eta_c(x)\delta\zeta \equiv s\eta\delta\zeta && (2.81)\\
\delta\psi(x) &= -gt_a\eta_a(x)\psi(x)\delta\zeta \equiv s\psi\delta\zeta && (2.82)\\
\delta\overline{\psi}(x) &= -g\overline{\psi}(x)t_a\eta_a(x)\delta\zeta \equiv s\overline{\psi}\delta\zeta && (2.83)
\end{aligned}$$

If we introduce source terms K and L for the operators sA and $s\eta$ respectively, performing the BRS transformation on the path integral gives

$$\begin{aligned}
&\int \mathcal{D}A\mathcal{D}\eta\mathcal{D}\overline{\eta}\mathcal{D}\psi\mathcal{D}\overline{\psi}\int d^4x\left(JsA+\overline{\omega}s\eta-\frac{1}{\xi}F\omega-g\overline{\sigma}\eta\psi+g\overline{\psi}\eta\sigma\right)(x)\\
&\qquad e^{-\int d^4y(\mathcal{L}^{YM}+\mathcal{L}^{GF}+\mathcal{L}^{FP})+J\cdot A+\overline{\omega}\cdot\eta+\overline{\eta}\cdot\omega+\overline{\psi}\cdot\sigma+\overline{\sigma}\cdot\psi} = 0 && (2.84)\\
\Rightarrow\ &\int d^4x\Big(J\frac{\delta}{\delta K}-\overline{\omega}\frac{\delta}{\delta L}-\frac{1}{\xi}\omega F[\frac{\delta}{\delta J}]\\
&\quad -\overline{\sigma}\frac{\delta^2}{\delta\overline{\omega}\delta\overline{\sigma}}+\frac{\delta^2}{\delta\sigma\delta\overline{\omega}}\Big)(x)e^W = 0 && (2.85)\\
\Rightarrow\ &\int d^4x\Big(J\frac{\delta}{\delta K}-\overline{\omega}\frac{\delta}{\delta L}-\frac{1}{\xi}\omega F[\frac{\delta}{\delta J}]\\
&\quad -\overline{\sigma}\frac{\delta^2}{\delta\overline{\omega}\delta\overline{\sigma}}+\frac{\delta^2}{\delta\sigma\delta\overline{\omega}}\sigma\Big)(x)W[J,\omega,\overline{\omega},K,L,\sigma,\overline{\sigma}] = 0 && (2.86)
\end{aligned}$$

Performing a Legendre transformation on this gives us

$$\int d^4x \left(\frac{\delta\Gamma}{\delta A}\frac{\delta\Gamma}{\delta K} + \frac{\delta\Gamma}{\delta\eta}\frac{\delta\Gamma}{\delta L} + \frac{\delta\Gamma}{\delta\psi}\left[\frac{\delta^2\Gamma}{\delta\eta\delta\psi}\right]^{-1} + \left[\frac{\delta^2\Gamma}{\delta\bar{\psi}\delta\eta}\right]^{-1}\frac{\delta\Gamma}{\delta\bar{\psi}} - \frac{1}{\xi}\frac{\delta\Gamma}{\delta\bar{\eta}}F[A]\right) = 0 \tag{2.87}$$

We can also, independently of this, perform a change of variables $\bar{\eta} \to \bar{\eta} + \delta\bar{\eta}$, which yields

$$\left(\omega(x) - \Phi\frac{\delta}{i\delta K(x)}\right) W[J,\omega,\bar{\omega},K,L] = 0 \tag{2.88}$$

$$\Rightarrow \quad \Phi^{\mu}_{ab}\frac{\delta\Gamma}{\delta K^{\mu}_b(x)} + \frac{\delta\Gamma}{\delta\bar{\eta}_a(x)} = 0 \tag{2.89}$$

where we have written

$$F_a(x) = \Phi^{\mu}_{ab}(x)A_{\mu b}(x) \tag{2.90}$$

For example, taking the derivative wrt $A(y)$ and $\eta(z)$ of (2.87) gives the Slavnov–Taylor equation for the gluon self-energy

$$\int d^4x \frac{\delta^2\tilde{\Gamma}}{\delta A^b_\nu(y)\delta A^a_\mu(x)}\frac{\delta^2\tilde{\Gamma}}{\delta\eta^c(z)\delta K^a_\mu(x)} = 0 \tag{2.91}$$

where $\tilde{\Gamma} = \Gamma - (1/2\xi)F^2$ and

$$\partial^{\mu}_x \frac{\delta^2\tilde{\Gamma}}{\delta\eta^c(z)\delta K^a_\mu(x)} + \frac{\delta^2\tilde{\Gamma}}{\delta\eta^c(z)\delta\bar{\eta}^a(x)} = 0, \tag{2.92}$$

follows from (2.89).

2.2 Renormalisation and counterterms

2.2.1 The principle of renormalisation

The (bare) parameters that enter into the action are not, in general, equal to those corresponding parameters that can be measured. The masses, kinetic terms and couplings will have contributions from self-interactions of the fields beyond what can naively be read out of the (bare) action. They will have to be renormalised, in order that the parameters we do put into the theory correspond to, or can be related to, measurable quantities. This is done by rewriting the theory in terms of the physical or renormalised parameters. In doing this, new terms — counterterms — will appear in the action. The theory is *renormalisable* if

1. only a finite number of counterterms are required
2. all the counterterms are local and Lorentz invariant
3. the bare and renormalised theories have the same symmetries

The last condition (which must be satisfied order by order in perturbation theory) leads to severe restrictions on the form the counterterms can take, since it means the Slavnov–Taylor identities must be satisfied order by order for gauge theories. It turns out that this can indeed be done. The Slavnov–Taylor identities guarantee the gauge invariance of the theory, in particular the universality of the coupling constant. If we write the counterterms as

$$\begin{aligned}
\Delta\mathcal{L} \;=\; & (Z_3-1)\frac{1}{2}\mathrm{Tr}[(\partial_\mu A_\nu - \partial_\nu A_\mu)^2] \\
& -g(Z_1-1)\mathrm{Tr}(\partial_\mu A_\nu - \partial_\nu A_\mu)[A_\mu, A_\nu]) \\
& +(Z_4-1)\frac{g^2}{2}Tr([A_\mu, A_\nu][A_\mu, A_\nu]) \\
& +(\tilde{Z}_3-1)(-\overline{\eta}_a\partial^2\eta_a) + g(\tilde{Z}_1-1)f_{abc}A^a_\mu\partial_\mu\overline{\eta}_b\eta_c \\
& +(Z_2-1)\overline{\psi}\partial\!\!\!/\psi + (Z_2\frac{m_0}{m}-1)m\overline{\psi}\psi
\end{aligned} \tag{2.93}$$

$$+ig(Z_{1F}-1)\overline{\psi}\gamma_\mu A_\mu \psi$$

then

$$\frac{Z_4}{Z_1} = \frac{Z_1}{Z_3} = \frac{\tilde{Z}_1}{\tilde{Z}_3} = \frac{Z_{1F}}{Z_2} \tag{2.94}$$

follows from the Slavnov–Taylor identities and guarantees that the renormalised coupling $g_R = Z_g g = Z_1 {Z_3}^{-3/2} g$ enters in the same way everywhere in the renormalised action. If we define the renormalised fields

$$A_\mu^R = Z_3^{-1/2} A_\mu^0 \tag{2.95}$$

$$\psi^R = Z_2^{-1/2} \psi^0 \tag{2.96}$$

$$\eta^R = \tilde{Z}_3^{-1/2} \eta^0 \tag{2.97}$$

the renormalised action takes the same form as the bare action, but with the renormalised fields and parameters rather than the bare ones entering.

In most quantum field theories, divergences will arise when evaluating Green functions perturbatively. Since the renormalised Green functions and parameters must be finite, this means that the bare parameters are infinite (or zero), and the infinities are absorbed into the counterterms. If this is to happen in a well-defined way, the theory must be regularised — which means that a momentum cutoff is imposed to make all quantities finite. In continuum calculations, this is normally done by dimensional regularisation, while the lattice automatically provides a momentum cutoff of π/a. A set of renormalisation conditions is then applied to the regularised Green functions. In dimensional regularisation, the most common scheme is the modified minimum subtraction scheme $\overline{MS}$, where only the divergent part and some associated terms are subtracted off. Although it is possible to implement an analogous minimal subtraction in lattice theories as well, momentum schemes, where the Green functions at some set of momenta are related to the tree level Green functions, are more appropriate and more commonly used.

The renormalisation constants will in general depend on all the defining parameters of the theory — coupling constants and masses — plus a scale that enters through the renormalisation. It is possible, and sometimes desirable, to choose a scheme where the dependence on for instance the masses is eliminated. The standard minimal subtraction scheme is such a mass-independent, but most lattice schemes are not, and it is considerably more complicated to disentangle the mass dependence in such schemes.

2.2.2 Renormalisation group and the QCD β-function

Consider a Green function

$$\begin{aligned}&\mathcal{G}_0^{(n)}(p_1,\ldots,p_{n_\psi},q_1,\ldots,q_{n_A};g_0,m_0)\\ &\quad= Z_2^{n_\psi/2}Z_3^{n_A/2}\mathcal{G}_R^{(n)}(p_1,\ldots,p_{n_\psi},q_1,\ldots,q_{n_A};g_R,m,\mu)\end{aligned}\tag{2.98}$$

and the associated proper Green function

$$\begin{aligned}&\Gamma_0^{(n)}(p_1,\ldots,p_{n_\psi},q_1,\ldots,q_{n_A};g_0,m_0)\\ &\quad= Z_2^{-n_\psi/2}Z_3^{-n_A/2}\Gamma_R^{(n)}(p_1,\ldots,p_{n_\psi},q_1,\ldots,q_{n_A};g_R,m,\mu)\end{aligned}\tag{2.99}$$

with n_ψ external fermion legs and n_A external gauge legs, in a mass-independent renormalisation scheme (so that we can simplify things by ignoring the masses). Since Γ_0 does obviously not depend on the renormalisation scale μ, we have

$$0=\mu\frac{\partial}{\partial\mu}\Gamma_0=\left[\mu\frac{\partial}{\partial\mu}+\beta(g)\frac{\partial}{\partial g}-n_A\gamma_A-n_\psi\gamma_\psi\right]\Gamma_R^{(n)}\tag{2.100}$$

which is the renormalisation group equation, with

$$\beta = \mu\frac{\partial g}{\partial\mu}\tag{2.101}$$

$$\gamma_A = Z_3^{-1/2}\mu\frac{\partial}{\partial\mu}Z_3^{1/2}\tag{2.102}$$

$$\gamma_\psi = Z_2^{-1/2}\mu\frac{\partial}{\partial\mu}Z_2^{1/2} \tag{2.103}$$

β can be calculated in perturbation theory, and to two loop order in a SU(N) gauge theory with N_f flavours, it is

$$\beta(g) = -b_0 g^3 - b_1 g^5 + \mathcal{O}(g^7) \tag{2.104}$$

$$b_0 = \frac{11N - 2N_f}{3(16\pi^2)} \tag{2.105}$$

$$b_1 = \frac{34N^2 - 10NN_f - 3N_f(N^2-1)/N}{3(16\pi^2)^2} \tag{2.106}$$

The coefficients b_0 and b_1 are scheme independent, as can be easily shown. If we call the renormalised coupling in one scheme g and in another scheme g_1, then we can expand g_1 in powers of g

$$g_1 = f(g) = g(1 + a_1 g^2 + \mathcal{O}(g^4)) \tag{2.107}$$

This gives

$$\begin{aligned}\beta_1(g_1) &= \mu\frac{\partial}{\partial\mu}f(g) = \mu\frac{\partial g}{\partial\mu}\frac{\partial f}{\partial g} \\ &= \beta(g)(1 + 3a_1 g^2 + \mathcal{O}(g^4)) \\ &= -b_0 g^3(1 + 3a_1 g^2) - b_1 g^5 + \mathcal{O}(g^7) \\ &= -b_0 g_1^3 - b_1 g_1^5 + \mathcal{O}(g_1^7)\end{aligned} \tag{2.108}$$

Integrating (2.101), and using (2.104), we find that

$$g^2(\mu) = \frac{g_0^2}{1+g_0^2 b_0 \ln(\mu^2/\mu_0^2)+g_0^2\frac{b_1}{b_0}\ln(1+g_0^2\ln(\mu^2/\mu_0^2)+g_0^2\frac{b_1}{b_0}\ln(b_0 g_0^2))} \tag{2.109}$$

where $g_0 = g(\mu_0)$. This can be rewritten in terms of a renormalisation group

invariant scale parameter Λ,

$$g^2(\mu) = \frac{1}{b_0 \ln(\mu^2/\Lambda^2) + \frac{b_1}{b_0} \ln\ln(\mu^2/\Lambda^2)} \tag{2.110}$$

where the scale parameter Λ is

$$\Lambda = \mu e^{-\frac{1}{2b_0 g^2(\mu)}} \left(b_0 g^2(\mu)\right)^{-\frac{b_1}{2b_0^2}} \tag{2.111}$$

Since g is not a scheme-independent quantity, Λ will also be different for different renormalisation schemes.

2.2.3 Lattice perturbation theory

Most of the discussion in the previous sections carries over directly to lattice gauge theories. In particular, if we add a discretised version of $\mathcal{L}^{GF}$ and $\mathcal{L}^{FP}$, as defined in (1.25) and (1.26) to the Wilson action $S_\Box + S^{WF}$, this can be shown to be invariant under BRS transformations defined in analogy to (2.79)-(2.83), and the effective action Γ satisfies the Slavnov–Taylor identities (2.87) and (2.89). This, and the renormalisability of lattice QCD to all orders in pertrubation theory, is worked out in detail by Reisz in [15].

Since numerical simulations are always performed using the bare fields and parameters, the renormalisation of the fields and couplings entering into the action will not be an issue when computing hadronic quantities. However, as will be explained below, the composite operators involved in hadronic physics also need to be renormalised, and their renormalisation constants have usually been computed perturbatively.

It turns out that perturbation series in $\alpha^{LAT} = g_0^2/4\pi = 3/2\pi\beta$, at least at the one-loop order, often give results in very poor agreement with experimental or non-perturbative determinations of the same quantities. This should not be a

surprise, since α^{LAT} is a bare quantity and perturbation series in the continuum are always expressed in terms of the renormalised coupling. If we re-express the perturbation series in terms of a renormalised coupling at some appropriate scale, it will be more well-behaved, as Lepage and Mackenzie [14] have shown.

2.3 Composite operators

In hadronic physics, we are interested in Green functions involving local operators composed of several quark and gluon fields: operators for creating and destroying mesons or baryons, electroweak currents, $K^0 - \overline{K^0}$ mixing operators, etc. These operators can be introduced into the partition function by coupling them to auxiliary sources, generating Green functions with operator insertions by taking derivatives with regard to the sources. Simple power counting will reveal that these insertions affect the degree of divergence of diagrams, possibly leading to new divergences which must be cancelled by new counterterms.[1] This will require new renormalisation conditions to be imposed on Green functions containing these operators.

When renormalising composite operators, it must be taken into account that they can mix with each other. Consider, for example, an operator $\mathcal{O}_1$ of dimension n. If there are other operators $\mathcal{O}_2, \ldots, \mathcal{O}_m$ with the same quantum numbers and with dimension $d \leq n$ (which must be compensated with factors a^{d-n}), these will in general mix with $\mathcal{O}_1$, so that the physical Green functions are linear combinations of the Green functions containing $\mathcal{O}_1, \ldots, \mathcal{O}_m$. The renormalised operator will

[1] Naively, one could expect that the renormalisation of the fields the operators are composed from is sufficient to cancel those divergences. However, this only renormalises the contributions from insertions of the kind $\Phi(x)\Phi(y)$, which involve 2 independent momenta, while a composite operator of the type $\Phi_a(x)\Phi_b(x)$ involves only one momentum. Alternatively, it can be argued that the composite operators (those whose renormalisation matters, at least) only appear in effective theories — eg, when the electroweak sector of the standard model is separated off, electroweak matrix elements are computed from Green functions containing current operators, bilinear in the quark fields.

then be

$$\mathcal{O}_1^R = \sum_{j=1}^{m} Z_{1j}\mathcal{O}_j \tag{2.112}$$

and similarly for the other operators. Alternatively, the operator can be redefined to subtract off the divergences from the lower-dimensional operators.

All these operators can be renormalised in perturbation theory the same way as the fields and parameters in the action, by evaluating Green functions with operator insertions to n-loop order and imposing renormalisation conditions. But sometimes higher-order or non-perturbative contributions to the renormalisation are significant, even when using a tadpole-improved scheme. It would therefore be useful to have a non-perturbative renormalisation procedure. Two such procedures are described below.

2.3.1 Chiral Ward identities and current renormalisation constants

We define the various lattice vector currents

$$V_\mu^{La}(x) = \overline{\psi}(x)\gamma_\mu\frac{1}{2}\lambda^a\psi(x) \tag{2.113}$$

$$V_\mu^{PSa}(x) = \frac{1}{2}\{\overline{\psi}(x+\hat{\mu})\gamma_\mu\frac{1}{2}\lambda^a U_\mu(x)\psi(x) + \text{h.c.}\} \tag{2.114}$$

$$\begin{aligned} V_\mu^{Ca}(x) = \frac{1}{2}\{&\overline{\psi}(x)(\gamma_\mu - r)U_\mu(x)\frac{1}{2}\lambda^a\psi(x+\hat{\mu}) \\ &+ \overline{\psi}(x+\hat{\mu})(\gamma_\mu + r)U_\mu^\dagger(x)\frac{1}{2}\lambda^a\psi(x)\} \end{aligned} \tag{2.115}$$

$$V_\mu^{CI\,a}(x) = V_\mu^{Ca}(x) + \frac{r}{2}\sum_\rho \partial_\rho(\overline{\psi}(x)\sigma_{\rho\mu}\frac{1}{2}\lambda^a\psi(x)), \tag{2.116}$$

the axial currents

$$A_\mu^{La}(x) = \overline{\psi}(x)\gamma_\mu\gamma_5\frac{1}{2}\lambda^a\psi(x) \tag{2.117}$$

$$A_\mu^{PSa}(x) = \frac{1}{2}\{\overline{\psi}(x+\mu)\gamma_\mu\gamma_5\frac{1}{2}\lambda^a U_\mu(x)\psi(x) + \text{h.c.}\}, \tag{2.118}$$

and the pseudoscalar and scalar densities

$$P^a(x) = \overline{\psi}(x)\gamma_5\frac{1}{2}\lambda^a\psi(x) \tag{2.119}$$

$$S^a(x) = \overline{\psi}(x)\frac{1}{2}\lambda^a\psi(x) \tag{2.120}$$

These are all flavour-mixing (non-singlet) currents; λ^a is a flavour SU(3) generator. The superscript 'PS' here denotes 'point split', while 'L' denotes 'local'. In the continuum limit, these operators are related to the physical operators by multiplicative renormalisation constants Z_V^L, Z_V^{PS}, Z_A^L etc, so that $V_\mu = Z_V^L V_\mu^L$ etc. The currents V_μ^C and V_μ^{CI} are both conserved, therefore their renormalisation constants are both 1, while the partial conservation of the local and point-split vector currents and axial currents guarantee that their renormalisation constants are finite. Z_P and Z_S are both infinite, but as we shall see, the Ward identities guarantee that the ratio Z_P/Z_S remains finite.

V_μ^{CI} is also improved according to the prescription in section 1.7.1. Thus the renormalisation constants for V_μ^L and V_μ^{PS} can be easily determined by evaluating

$$Z_V^{L,PS} = \frac{\langle\alpha\,|\,V_\mu^{CI}(x)\,|\,\beta\rangle}{\langle\alpha\,|\,V_\mu^{L,PS}(x)\,|\,\beta\rangle} \tag{2.121}$$

between arbitrary hadron states $\langle\alpha|$ and $|\beta\rangle$. Alternatively, they may be determined from

$$Z_V^{L,PS} = \frac{\sum_{\vec{x}}\langle P^\dagger(0)P(\vec{x},T)\rangle}{\sum_{\vec{x},\vec{y}}\langle P^\dagger(0)V_4^{L,PS}(\vec{y},t)P(\vec{x},T)\rangle} \tag{2.122}$$

This should give a precise estimate provided the effect of the off-diagonal matrix elements $\langle P_m\,|\,V_4^{L,PS}\,|\,P_n\rangle$ can be neglected, since, if we write

$$\begin{aligned} C^{3pt} &= \sum_{\vec{x},\vec{y}}\Big\langle P^\dagger(0)V_4(\vec{y},t)P(x,T)\Big\rangle \\ &= \sum_{\vec{x},\vec{y}}\sum_{m,n}\frac{1}{2E_m}\frac{1}{2E_n}\langle 0\,|\,P^\dagger(0)\,|\,P_m\rangle\langle P_m\,|\,V_4(\vec{y},t)\,|\,P_n\rangle \end{aligned}$$

$$\begin{aligned}
&\langle P_n \mid P(\vec{x},T) \mid 0\rangle \\
&= \sum_{m,n} \frac{C_m}{2E_m} \sum_{\vec{y}} \langle P_m \mid V_4(0) e^{-i(\vec{p}_m - \vec{p}_n)\vec{y}} e^{-(E_m - E_n)t} \mid P_n\rangle \frac{C_n}{2E_n} e^{-E_n T} \\
&= \sum_{m,n} \frac{C_m C_n}{(2E_m)(2E_n)} \langle P_m \mid V_4(0) \mid P_n\rangle e^{-E_n T} e^{-(E_m - E_n)t} \qquad (2.123)
\end{aligned}$$

and

$$C^{2pt} = \sum_{\vec{x}} \left\langle P^\dagger(0) P(\vec{x},T) \right\rangle = \sum_n \frac{C_n^2}{2E_n} e^{-E_n T} \qquad (2.124)$$

then, since $\langle P_n \mid V_4(0) \mid P_n\rangle = 2E_n/Z_V$ for degenerate mesons, it follows that $C^{3pt} = C^{2pt}/Z_V$ if we ignore the off-diagonal elements. For non-degenerate mesons, we have instead $C^{3pt} = C^{2pt}/2Z_V$, since in this case $\langle P_n \mid V_4(0) \mid P_n\rangle = E_n/Z_V$.

Ward identities with the standard Wilson action

For the axial case, there is no conserved current or other "easy" way of determining the renormalisation constants, but they can be obtained using chiral Ward Identities. If we define the transformations

$$\delta_A \psi(x) = i\alpha^a(x) \frac{1}{2} \lambda^a \gamma_5 \psi(x) \qquad \delta_A \overline{\psi}(x) = i\alpha^a(x) \overline{\psi}(x) \frac{1}{2} \lambda^a \gamma_5, \qquad (2.125)$$

equation (2.73), with $\omega(x) = \alpha^a(x)$, becomes[2]

$$\begin{aligned}
i \left\langle \frac{\delta O(x_1, x_2, \cdots)}{\delta \alpha^a(x)} \right\rangle &= \left\langle \partial_x^\mu A_\mu^a O(x_1, x_2, \cdots) \right\rangle \\
&- \left\langle O(x_1, x_2, \cdots) [\overline{\psi}(x) \{\frac{1}{2}\lambda^a, M_0\} \gamma_5 \psi(x) + X^a(x)] \right\rangle \qquad (2.126)
\end{aligned}$$

where M_0 is the bare mass matrix and $X^a(x)$ is the chiral variation of the Wilson term of the action. This is a dimension-5 operator that is equal to zero at tree

[2]The Ward identities that naturally come out of this are expressed in terms of the point-split currents and the forward lattice derivative. However, if we replace the forward by the symmetric derivative and point-split by local currents, the resulting Ward identities only differ by terms of $O(a^2)$.

level in the continuum limit, but it mixes with $\partial_\mu A^a_\mu$ and $\overline{\psi}\lambda^a\gamma_5\psi$, so we define, following [16],

$$\overline{X}^a = X^a + \{\frac{1}{2}\lambda^a, \overline{M}\}P^a + (Z_A - 1)\partial_\mu A^a_\mu \tag{2.127}$$

Requiring that $\langle\alpha\,|\,\overline{X}^a\,|\,\beta\rangle = 0$ for all on-shell $\langle\alpha|$ and $|\beta\rangle$ determines

$$\rho = \frac{m}{Z_A} = \frac{M_0 + \overline{M}}{Z_A} = \frac{\langle 0\,|\,\partial_4 A^a_4\,|\,P^a\rangle}{2\langle 0\,|\,P^a\,|\,P^a\rangle} \tag{2.128}$$

where ρ, m and $\overline{M}$ are in general matrices in flavour space. If we set $\mathcal{O}(y,0) = A^{Lb}_\nu(y)V^{Lc}_\rho(0)$ and assume all quark masses are degenerate, (2.126) can be re-ordered to yield [16]

$$\begin{aligned}
&\partial^\mu_x\langle\hat{A}^a_\mu(x)\hat{A}^b_\nu(y)\hat{V}^c_\rho(0)\rangle = \\
&\quad\langle\overline{X}^a(x)\hat{A}^b_\nu(y)\hat{V}^c_\rho(0)\rangle + \langle\overline{\psi}(x)\{\frac{1}{2}\lambda^a, m\}\gamma_5\psi(x)\hat{A}^b_\nu(y)\hat{V}^c_\rho(0)\rangle \\
&+\; if^{abd}\delta(x-y)\frac{Z_A}{Z_V}\langle\hat{V}^d_\nu(y)\hat{V}^c_\rho(0)\rangle \\
&+\; if^{acd}\delta(x)\frac{Z_V}{Z_A}\langle\hat{A}^b_\nu(y)\hat{A}^d_\rho(0)\rangle
\end{aligned} \tag{2.129}$$

where $\hat{A} = Z^L_A A^L$ and $\hat{V} = Z^L_V V^L$ are the operators with the correct continuum limit. The continuum Ward identity

$$\begin{aligned}
&\partial^\mu_x\langle A^a_\mu(x)A^b_\nu(y)V^c_\rho(0)\rangle = \\
&\quad\langle\overline{\psi}(x)\{\frac{1}{2}\lambda^a, m\}\gamma_5\psi(x)A^b_\nu(y)V^c_\rho(0)\rangle \\
&+\; if^{abd}\langle V^d_\nu(y)V^c_\rho(0)\rangle + if^{acd}\delta(x)\langle A^b_\nu(y)A^d_\rho(0)\rangle
\end{aligned} \tag{2.130}$$

is recovered if

$$\begin{aligned}
&\langle\xi^{La}(x)A^{Lb}_\nu(y)V^{Lc}_\rho(0)\rangle = \\
&\quad if^{abd}\frac{Z^L_V}{{Z^L_A}^2}\delta(x-y)\langle V^{Ld}_\nu(y)V^{Lc}_\rho(0)\rangle \\
&+\; if^{acd}\frac{1}{Z^L_V}\delta(x)\langle A^{Lb}_\nu(y)A^{Ld}_\rho(0)\rangle
\end{aligned} \tag{2.131}$$

where

$$\xi^{La}(x) = \partial^\mu A_\mu^{La}(x) - 2\rho P^a(x) \tag{2.132}$$

Similarly, setting $O(y,0) = S^b(y)P^c(0)$ we obtain

$$\begin{aligned}\langle \xi^{La}(x) S^b(y) P^c(0)\rangle = \\ - \; d^{abd}\frac{Z_P}{Z_A^L Z_S}\delta(x-y)\langle P^d(y)P^c(0)\rangle \\ - \; d^{acd}\frac{Z_S}{Z_A^L Z_P}\delta(x)\langle S^b(y)S^d(0)\rangle\end{aligned} \tag{2.133}$$

where d^{abc} is defined by

$$\{\lambda^a, \lambda^b\} = 2d^{abc}\lambda^c + \frac{4}{N_f}\delta^{ab}$$

This equation can be used to obtain the ratio of the scalar and pseudoscalar density renormalisation constants Z_S/Z_P.

Ward identities with the improved action

The derivation of the Ward identities for the SW action is practically identical to the derivation for the Wilson action. However, further complications are brought in by the improved operators. Bilinear improved operators can be obtained [17] by replacing $\overline{\psi}(x)\Gamma\psi(x)$ with $\overline{\psi}(x)(1 + \frac{ra}{4}(\overleftarrow{\not{D}} + m_0))\Gamma(1 - \frac{ra}{4}(\not{D} - m_0)) \equiv \overline{\psi}(x)\tilde{\Gamma}\psi(x)$.

The terms involving m_0 can be eliminated using the equations of motion

$$(\not{D} + m_0)S(x,y) = \delta(x-y) \qquad S(x,y)(\overleftarrow{\not{D}} - m_0) = -\delta(x-y) \tag{2.134}$$

where S is the quark propagator. Inserting this into the LHS of (2.131), we get

$$\langle P^a(x) A_\nu^{Lb}(y) V_\rho^{Lc}(0)\rangle$$

$$
\begin{aligned}
&= \langle\overline{\psi}(x)\,\tilde{\Gamma}^a_5\,\psi(x)\overline{\psi}(y)\,\tilde{\Gamma}^b_{A\nu}\,\psi(y)\overline{\psi}(0)\,\tilde{\Gamma}^c_{V\rho}\,\psi(0)\rangle \\
&= -\langle \mathrm{Tr}S(0,x)\,\tilde{\Gamma}^a_5\,S(x,y)\,\tilde{\Gamma}^b_{A\nu}\,S(y,0)\,\tilde{\Gamma}^c_{V\rho}\rangle \\
&\quad -\langle \mathrm{Tr}S(y,x)\,\tilde{\Gamma}^a_5\,S(x,0)\,\tilde{\Gamma}^c_{V\rho}\,S(0,y)\,\tilde{\Gamma}^c_{A\nu}\rangle \\
&= -\langle \mathrm{Tr}S(0,x)\,\hat{\Gamma}^a_5\,S(x,y)\,\hat{\Gamma}^b_{A\nu}\,S(y,0)\,\hat{\Gamma}^c_{V\rho}\rangle \\
&\quad -\langle \mathrm{Tr}S(y,x)\,\hat{\Gamma}^a_5\,S(x,0)\,\hat{\Gamma}^c_{V\rho}\,S(0,y)\,\hat{\Gamma}^c_{A\nu}\rangle \\
&\quad +\frac{ra}{2}if^{acd}\delta(x)\langle \mathrm{Tr}S(0,y)\,\hat{\Gamma}^b_{A\nu}\,S(y,0)\,\hat{\Gamma}^d_{A\rho}\rangle \\
&\quad +\frac{ra}{2}if^{abd}\delta(x-y)\langle \mathrm{Tr}S(0,y)\,\hat{\Gamma}^d_{V\nu}\,S(y,0)\,\hat{\Gamma}^c_{V\rho}\rangle \\
&\quad +\text{terms at } y=0
\end{aligned}
$$

where

$$\hat{\Gamma} \equiv (1+\frac{ra\overleftarrow{\not{D}}}{2})\Gamma(1-\frac{ra}{2}\not{D})$$

So if we sum over all x and spatial $\vec{y}$ (keeping $y \neq 0$) in eq. (2.131), we obtain

$$
\begin{aligned}
&2\rho\sum_{x,\vec{y}}\langle P^a(x)A^{Lb}_\nu(y)V^{Lc}_\rho(0)\rangle \\
&= -i(\frac{Z^L_V}{Z^{L\,2}_A}-\rho ra)f^{abd}\sum_{\vec{y}}\langle V^{Ld}_\nu(y)V^{Lc}_\rho(0)\rangle \\
&\quad -i(\frac{1}{Z^L_V}-\rho ra)f^{acd}\sum_{\vec{y}}\langle A^{Lb}_\nu(y)A^{Ld}_\rho(0)\rangle
\end{aligned}
\tag{2.135}
$$

Similarly, (2.133) becomes

$$
\begin{aligned}
&2\rho\sum_{x,\vec{y}}\langle P^a(x)S^b(y)P^c(0)\rangle \\
&= (\frac{Z_P}{Z^L_A Z_S}-\rho ra)d^{abd}\sum_{\vec{y}}\langle P^d(y)P^c(0)\rangle \\
&\quad (\frac{Z_S}{Z^L_A Z_P}-\rho ra)d^{acd}\sum_{\vec{y}}\langle S^b(y)S^d(0)\rangle
\end{aligned}
\tag{2.136}
$$

2.3.2 Renormalisation with quark Green functions

Another, more generally applicable method for non-perturbative renormalisation of operators is by imposing conditions on matrix elements of the operators between quark Green functions [18]. This method requires gauge fixing, since the quark Green functions are gauge dependent quantities, but has the advantage that the scheme is defined in the continuum as well as on the lattice, so that matching to commonly used continuum schemes is straightforward. The conditions imposed are also of the same kind as you would naturally choose in lattice perturbation theory.

More precisely, the renormalised Green function $\mathcal{G}_{\mathcal{O}}^{R}(pa)$ of the operator $\mathcal{O}$ computed between between quark states $\mid pa\rangle$ at a chosen momentum is fixed to its tree-level value

$$\mathcal{G}_{\mathcal{O}}^{R}(pa) = Z_{\mathcal{O}}(\mu a)\langle pa \mid \mathcal{O} \mid pa\rangle|_{p^2=\mu^2} = \langle p \mid \mathcal{O} \mid p\rangle_0 \tag{2.137}$$

In practice, this is done by fixing the renormalised proper Green function $\Gamma_{\mathcal{O}}(pa)$ to 1

$$Z_{\mathcal{O}}(\mu a)Z_2^{-1}(\mu a)\Gamma_{\mathcal{O}}(pa)|_{p^2=\mu^2} = 1 \tag{2.138}$$

where

$$\Gamma_{\mathcal{O}}(pa) = \frac{1}{12}\mathrm{Tr}\left(S(pa)^{-1}\mathcal{G}_{\mathcal{O}}(pa)S(pa)^{-1}P_{\mathcal{O}}\right) \tag{2.139}$$

$P_{\mathcal{O}}$ is a projector onto the tree-level operator. The quark field renormalisation constant Z_2 can be defined, for instance by requiring that the quark propagator equals the tree-level propagator

$$Z_2(\mu) = \left.\frac{\mathrm{Tr}\left(-i\sum_\nu \gamma_\nu \sin(p_\nu a)S^{-1}(pa)\right)}{4\sum_\nu \sin^2(p_\nu a)}\right|_{p^2=\mu^2} \tag{2.140}$$

or by requiring that Z_V^C, computed in this scheme, is equal to 1.

Chapter 3

Renormalisation of current operators

3.1 Computational details

The results reported in this chapter have been obtained using the Wilson gauge action (1.43) and SW fermion action (1.66), in the quenched approximation. The configurations were generated using the Hybrid Over-Relaxed algorithm, described in [19], on a $16^3 \times 48$ lattice at $\beta = 6.0$ and a $24^3 \times 48$ lattice at $\beta = 6.2$. At $\beta = 6.2$, the configurations were separated by 2400 sweeps, after an initial thermalisation of 16800 sweeps. The configurations at $\beta = 6.0$ were separated by 1200 sweeps, after a thermalisation of 10800 sweeps.

The propagators used are the same as in [30] for $\beta = 6.2$ and [20] for $\beta = 6.0$, except for the tadpole improved and heavy quark propagators in section 3.3, which were generated specifically for the purpose of this analysis. They were all generated using point sources and sinks. The details of the algorithm used are described in [19].

Since we normally only compute propagators from the origin to any point in space and time, the 3-point functions in (2.122), (2.135) and (2.136) could not be evaluated directly from the existing data. Instead, 'extended propagators' $S_1(y,0) = \sum_x S(y,x)\gamma_5 S(x,0)$ and $S_1'(y,0;T) = \sum_{\vec{x}} S(y,\vec{x},T)\gamma_5 S(\vec{x},T,0)$ were

generated using

$$M_{zy}S_1(y,0) = \gamma_5 S(z,0) \tag{3.141}$$

$$M_{zy}S_1'(y,0) = \gamma_5 S(z,0)\delta_{t_z T} \tag{3.142}$$

$$\tag{3.143}$$

The code to initialise the solver for (3.141) was written specifically for this study.

The statistical analysis has been performed using minimum χ^2 fits to the time-sliced data, using both correlated and uncorrelated χ^2's. The errors were obtained by a bootstrap procedure, using 100 bootstrap samples.

3.2 The ρ parameter

Using the property of the Wilson propagator

$$S(0,x) = \gamma_5 S^\dagger(x,0)\gamma_5 \tag{3.144}$$

and the zero-momentum pseudoscalar ground state

$$|P\rangle = \sum_{\vec{x}} P(\vec{x},0)|0\rangle \tag{3.145}$$

we find that ρ, defined in (2.128), can be estimated by

$$\rho(t) = \frac{\partial_0 \sum_{\vec{x}} S^\dagger(\vec{x},t;0)\gamma_0 S(\vec{x},t;0)}{2\sum_{\vec{x}} S^\dagger(\vec{x},t;0)S(\vec{x},t;0)} \tag{3.146}$$

where ∂_4 is the symmetric derivative

$$\partial_\mu f(x) = \frac{f(x+\hat{\mu}) - f(x-\hat{\mu})}{2} \tag{3.147}$$

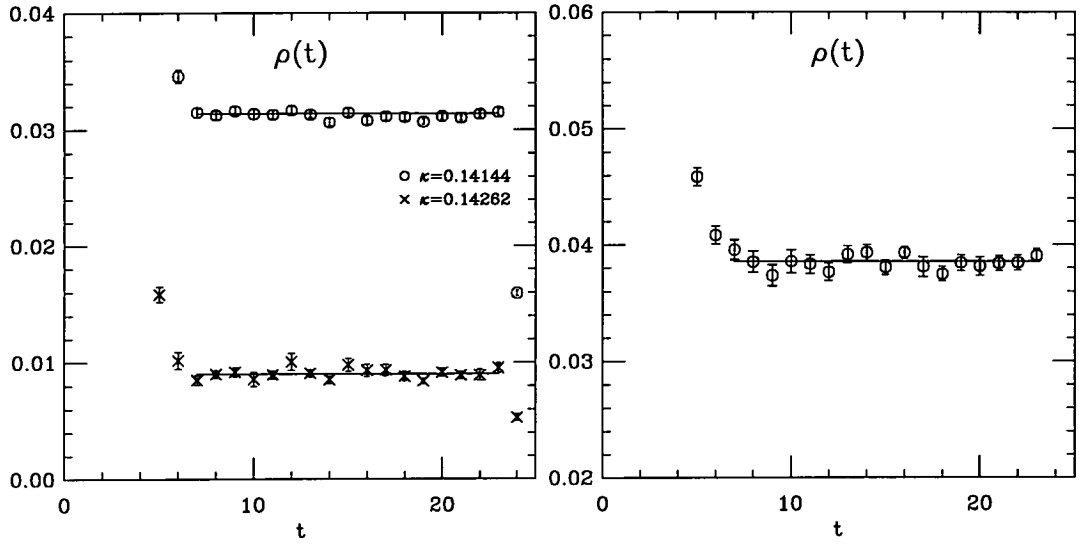

Figure 3.1: ρ as a function of t (in lattice units), for $\beta = 6.2$ (left) and $\beta = 6.0$ (right).

β	κ	m_{PS}^2 (GeV^2)	ρa
6.2	0.14262	0.208(7)	$0.00903\ ^{+\ 12}_{-\ 18}$
	0.14144	0.663(7)	$0.03141\ ^{+\ 11}_{-\ 20}$
6.0	0.1432	0.615(10)	$0.03849\ ^{+\ 28}_{-\ 37}$

Table 3.1: Values of the ρ parameter, in lattice units, as a function of the quark mass.

$\rho(t)$ was computed for 60 configurations at β=6.2, with κ=0.14144 and 0.14262, and for 36 configurations at β=6.0, κ=0.1432. The results are shown in figure 3.1. From these plots we see that ρ is constant between $t = 7$ and $t = 23$ approximately. Fitting $\rho(t)$ to a constant between timeslices 7 and 23 also give the best values for χ^2 per degree of freedom (fitting between timeslices 7 and 22 gives a slightly better χ^2 for the data at $\beta = 6.0$, but this is marginal), so these are the values quoted in table 3.1 and used subsequently.

3.3 Vector current

3.3.1 Standard SW action

Z_V was determined from eq. (2.122), using 10 configurations, at three values for the quark mass for $\beta = 6.2$ (corresponding to $\kappa = 0.14144$, $\kappa = 0.14226$ and $\kappa = 0.14262$), and at $\kappa = 0.1432$ for $\beta = 6.0$. The results are presented as a function of t in figs.3.2 and 3.3. We see that the values for Z_V are roughly independent of t, as one would expect from (2.123). The best values, obtained by fitting to timeslices 5–19, are given in table 3.2. The errors from the variation between the timeslices are obtained from fits to 100 bootstrap samples of timeslices within this fitting range.

The results are plotted as a function of the square of the mass of the pseudoscalar meson (proportional to the quark mass) in fig.3.4. We see that the results show a clear (linear) dependence on the quark mass. Since this renormalisation scheme is not explicitly mass independent, one would expect that the improved, renormalised current takes the form [11] $V_R = Z_V(1 + b_V am)V$. The parameter b_V is currently not known, even to tree level. The mass dependence is also consistent with the expectation that the leading corrections to these calculations should be of $O(\alpha_s m_0 a)$. Perturbation theory at one-loop level [22, 23] with a mean-field rescaled coupling constant $\beta' = \beta/u_0^4$ gives $Z_V^L = 0.842$ which is quite close to, but still incompatible with, these non-perturbative values. The result for β=6.0 is also in good agreement with the values quoted in [24], which are obtained using a slightly different method.

Z_V^L has also been determined from eq. (2.135), with $\nu = \rho = 0$ (using that $\langle V_\nu(y)V_\rho(0)\rangle = 0$ to simplify the expression), at κ=0.14144 (β=6.2) and κ=0.1432 (β=6.0). This gives $Z_V^L = 0.817\ ^{+\ 8}_{-\ 10}$ at β=6.2, and $Z_V^L = 0.801\ ^{+\ 10}_{-\ 8}$ at β=6.0. Both these values are within 2σ of the results obtained from eq. (2.122).

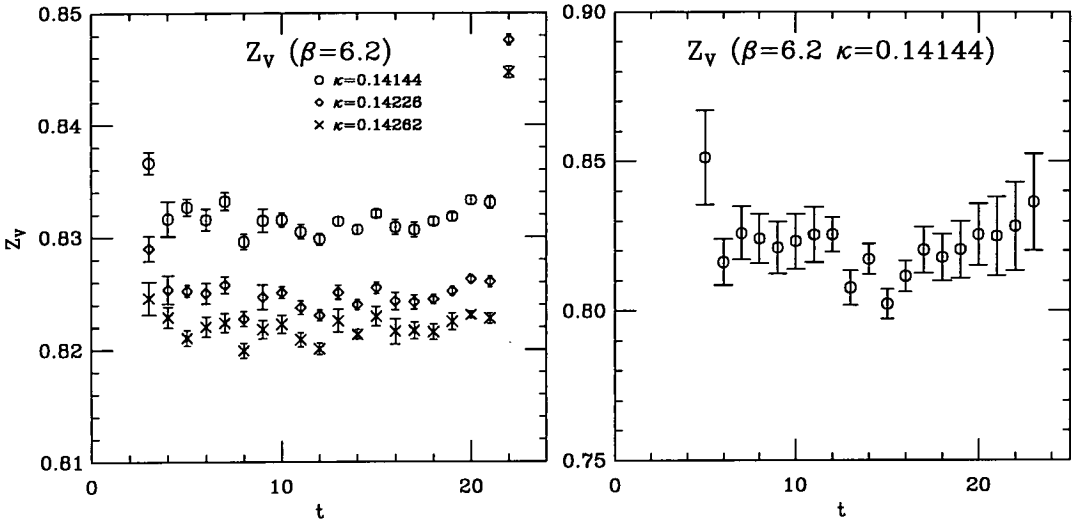

Figure 3.2: Z_V^L as a function of t, using the ratio (2.122) (left), and for $\kappa = 0.14144$, using the Ward identity (2.135) (right).

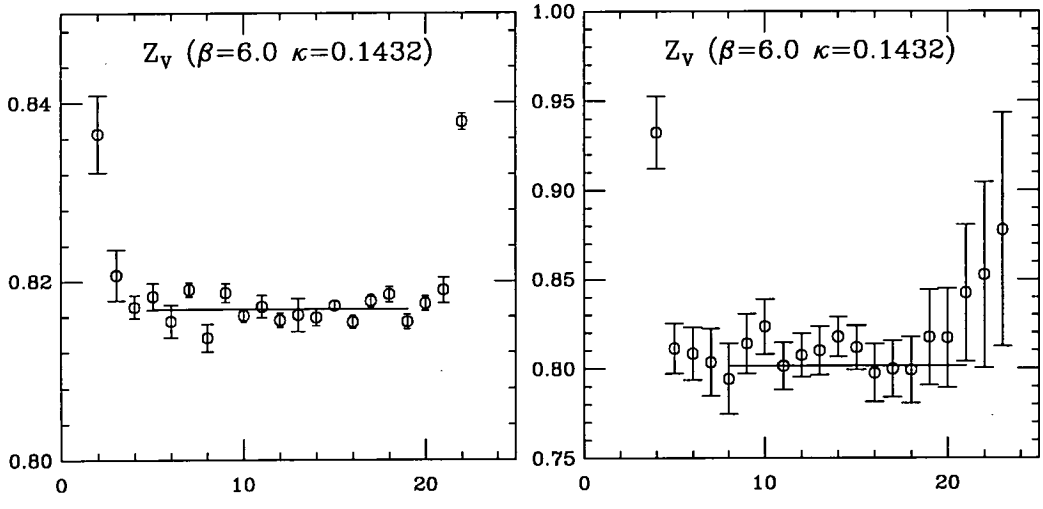

Figure 3.3: Z_V^L as a function of t, for $\beta = 6.0$, $\kappa = 0.1432$, using the ratio (2.122) (left), and using the Ward identity (2.135) (right).

3.3.2 Tadpole improved action

In an attempt to investigate the effect and viability of tadpole improvement, Z_V was computed for mesons composed of two heavy quarks and of one heavy and one light quark, for a 'standard' and a tadpole improved SW action at $\beta = 6.0$.

β	κ	m_{PS}^2	Z_V^L
6.2	0.14262	0.208	$0.82139\ ^{+\ 41}_{-\ 12}\ ^{+\ 25}_{-\ 25}$
	0.14226	0.341	$0.82453\ ^{+\ 24}_{-\ 22}\ ^{+\ 24}_{-\ 23}$
	0.14144	0.663	$0.83136\ ^{+\ 23}_{-\ 16}\ ^{+\ 22}_{-\ 23}$
6.0	0.1432	0.615	$0.81683\ ^{+\ 45}_{-\ 33}$

Table 3.2: Values of the renormalisation constant Z_V^L as a function of the quark mass. The first set of errors are the statistical errors, while the second set are the errors due to the variation between the timeslices.

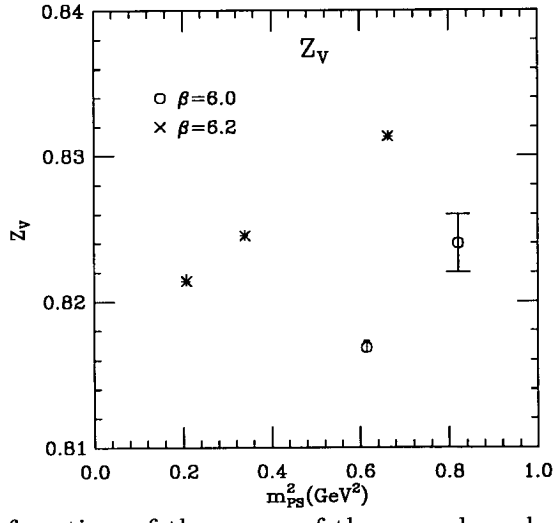

Figure 3.4: Z_V^L as a function of the mass of the pseudoscalar meson. The heavier point at β=6.0, taken from [21], is included for comparison.

The tadpole improvement was implemented by replacing $U_\mu(x)$ with $U_\mu(x)/u_0$, with $u_0 = 0.87779$, before computing the propagators.

It was expected that tadpole improvement would bring about better agreement between non-perturbative perturbative results. In particular, since to one-loop order Z_V is supposed to be mass-independent, tadpole improvement should reduce the mass dependence observed here and in [25].

Another effect of tadpole improvement should be that the current quark mass used in the definition of improved operators is more well-defined. If we write

$$\hat{\Gamma} = (1 + (1-z)ar\tilde{m}_0)\left(1 + z\frac{ar\overleftarrow{\not{D}}}{2}\right)\Gamma\left(1 - z\frac{ar}{2}\not{D}\right) \tag{3.148}$$

the equations of motion can be used to eliminate either $\tilde{m}_0(z = 1)$ or $\not{D}(z = 0)$. The latter would be considerably cheaper computationally, but depends on a reliable estimate of the 'bare' (subtracted) quark mass $\tilde{m}_0$. Using a tadpole improved action will bring κ_c closer to its tree-level value of 1/8, and tadpole perturbation theory could then provide an estimate of $\tilde{m}_0$, or the dependence of quantities like $\tilde{Z}_V$ on $\tilde{m}_0$.

In this study, $\tilde{Z}_V = \tilde{C}^{2pt}/\tilde{C}^{3pt}$, where $\tilde{C}^{2pt,3pt}$ are the unrotated (unimproved) correlators, is computed, and $Z_V^{z=0}$ is obtained from

$$Z_V^{z=0} = (1 + am_p)\tilde{Z}_V \tag{3.149}$$

where $m_p = \ln(1 + m_0 - m_c) = \ln(1 + \frac{1}{2\kappa} - \frac{1}{2\kappa_c})$ is the (heavy) quark pole mass.

For the data without tadpole improvement, κ values of 0.133, 0.125 and 0.111 were used for the heavy quarks. For the tadpole improved data, $\kappa = 0.11411, 0.1095$ and 0.096 were used for the heavy quarks, and $\kappa = 0.1210$ and 0.1218 for the light quarks. The lightest quark was only used to create degenerate light mesons, in order to obtain an estimate for κ_c — all the heavy–light mesons had $\kappa_l = 0.1210$.

The pseudoscalar mass was extracted using uncorrelated fits to timeslices 10 to 19 (5 to 19 for the tadpole improved $z = 1$ data). Using the data from the two light quarks, the critical hopping parameter was found to be $\kappa_c = 0.12235$.

The results are presented in tables 3.3 and 3.4. All the rotated results are obtained with a sample of 10 configurations. The heavy–heavy and light–light unrotated results are also obtained with 10 configurations, while the heavy–light results are from 15 configurations. All the data are shown as a function of the heavy quark pole mass m_p in fig.3.7.

	Heavy–heavy		Heavy–light	
κ_h	$m_{PS}a$	Z_V	$m_{PS}a$	Z_V
0.133	$1.020\ ^{+\ 5}_{-\ 4}$	$0.9022\ ^{+\ 4}_{-\ 5}$	$0.733\ ^{+\ 10}_{-\ 6}$	$0.8921\ ^{+\ 6}_{-\ 7}$
0.125	$1.409\ ^{+\ 4}_{-\ 4}$	$0.9602\ ^{+\ 3}_{-\ 5}$	$0.947\ ^{+\ 10}_{-\ 7}$	$0.9458\ ^{+\ 6}_{-\ 8}$
0.111	$2.013\ ^{+\ 3}_{-\ 3}$	$1.0391\ ^{+\ 4}_{-\ 3}$	$1.274\ ^{+\ 11}_{-\ 8}$	$1.0178\ ^{+\ 11}_{-\ 15}$

Table 3.3: Z_V for heavy–heavy and heavy–light mesons, using the standard SW action.

As fig.3.7 shows, tadpole improvement does reduce the mass dependence of Z_V, although there is still a significant mass dependence left. This is not surprising, since the SW action is only tree level improved, and $\mathcal{O}(\alpha_s ma)$ errors may still be

		$z = 0$			$z = 1$	
κ_1	κ_2	$m_{PS}a$	Z_V	Z_V	$m_{PS}a$	Z_V
0.12100	0.12100	0.334(8)	$0.8957\ ^{+\ 3}_{-\ 4}$	$0.8576\ ^{+\ 3}_{-\ 4}$	0.332(7)	$0.9437\ ^{+\ 4}_{-\ 5}$
0.12180	0.12180				0.21(1)	$0.9367\ ^{+\ 8}_{-\ 7}$
0.12100	0.11411	0.665(8)	$1.133\ ^{+\ 5}_{-\ 6}$	$0.900\ ^{+\ 5}_{-\ 6}$	0.671(8)	$0.964\ ^{+\ 2}_{-\ 2}$
	0.10950	0.834(8)	$1.360\ ^{+\ 2}_{-\ 3}$	$0.977\ ^{+\ 2}_{-\ 3}$	0.841(9)	$1.016\ ^{+\ 1}_{-\ 1}$
	0.09600	1.24(1)	$2.054\ ^{+\ 6}_{-\ 6}$	$1.172\ ^{+\ 6}_{-\ 6}$	1.25(1)	$1.079\ ^{+\ 2}_{-\ 3}$
0.11411	0.11411	0.932(7)	$1.179\ ^{+\ 1}_{-\ 2}$	$0.9365\ ^{+\ 11}_{-\ 14}$	0.933(6)	$1.0010\ ^{+\ 5}_{-\ 6}$
0.10950	0.10950	1.237(5)	$1.385\ ^{+\ 1}_{-\ 1}$	$0.9953\ ^{+\ 12}_{-\ 10}$	1.238(4)	$1.0334\ ^{+\ 4}_{-\ 6}$
0.09600	0.09600	1.982(3)	$2.107\ ^{+\ 1}_{-\ 1}$	$1.2023\ ^{+\ 10}_{-\ 11}$	1.983(3)	$1.1016\ ^{+\ 4}_{-\ 7}$

Table 3.4: Z_V for light–light, heavy–light, and heavy–heavy mesons, using rotated and unrotated tadpole improved propagators. The errors are purely statistical.

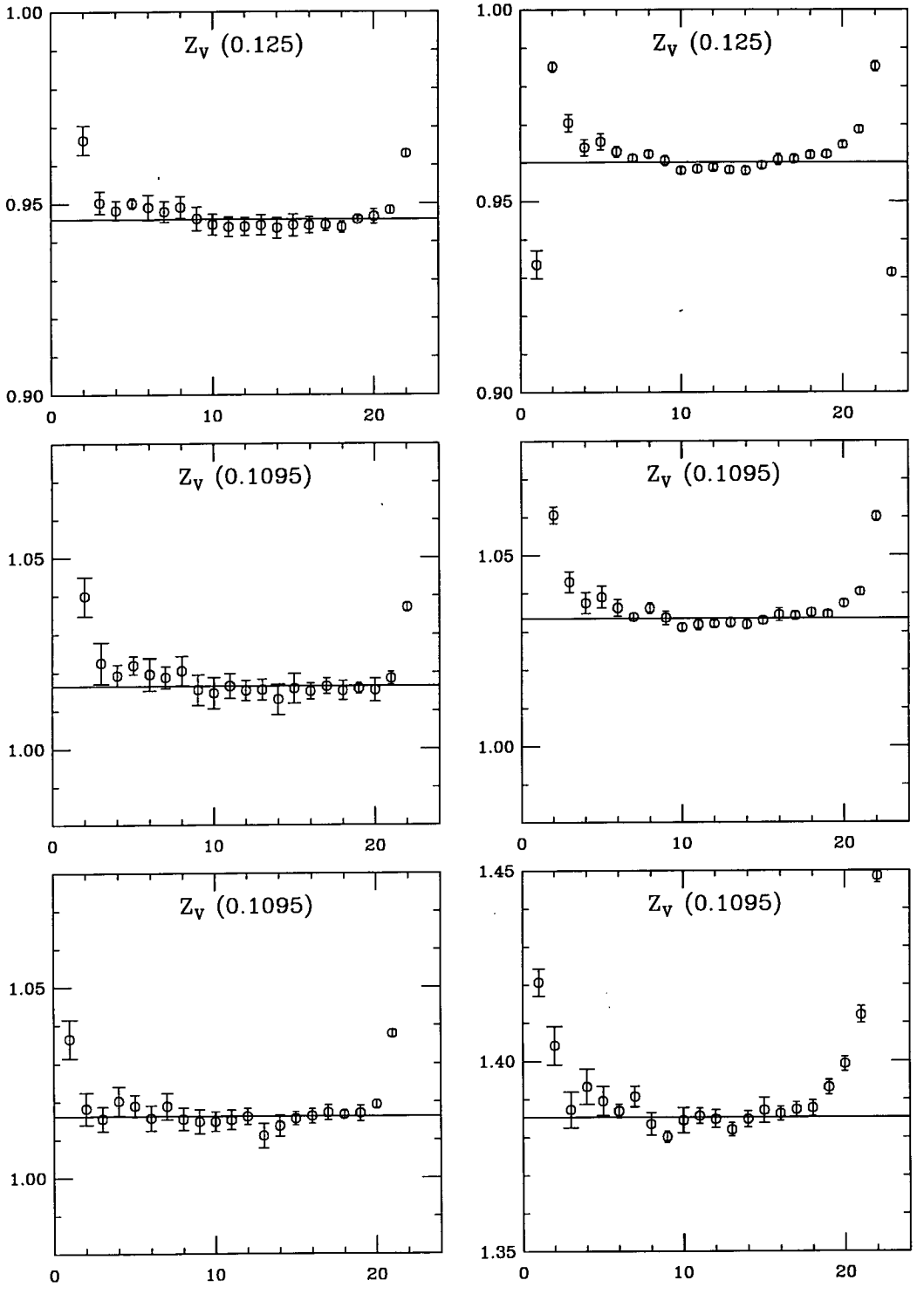

Figure 3.5: The vector current renormalisation constant as a function of t, for $\beta = 6.0$, heavy–light mesons (left) and heavy–heavy mesons (right). The top figures are data without tadpole improvement, the middle figures for tadpole improved data with $z = 1$, and the bottom figures show $\tilde{Z}_V$ for tadpole improved data with $z = 0$.

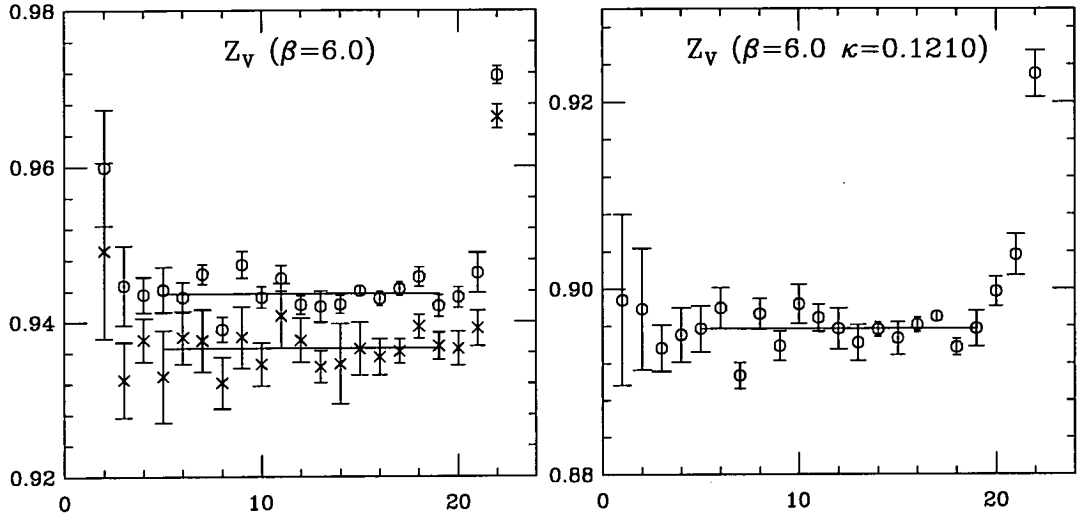

Figure 3.6: Z_V^L as a function of t for rotated (left) and unrotated (right) light mesons.

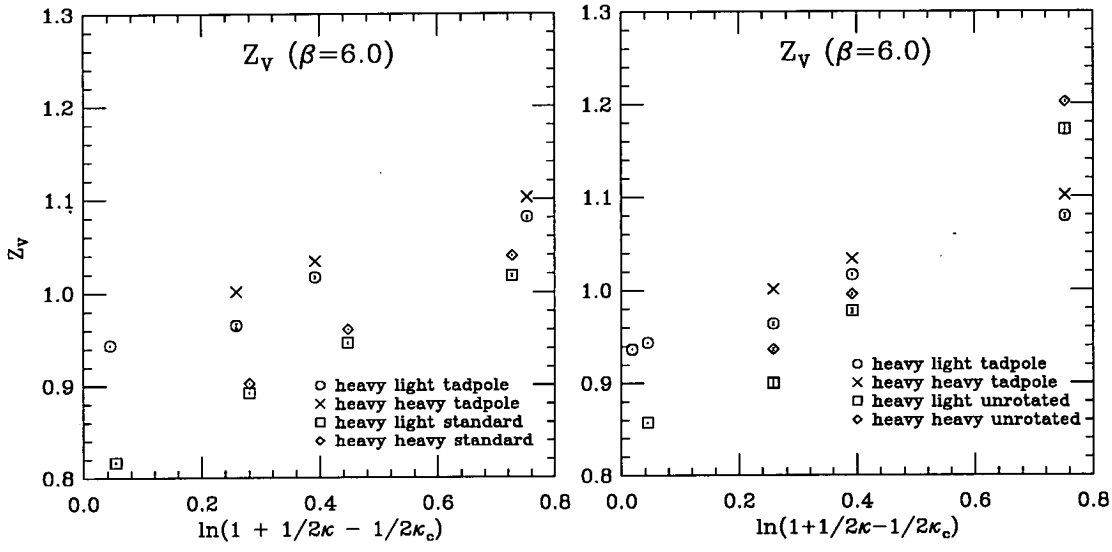

Figure 3.7: Z_V^L as a function of the heavy quark pole mass, comparing tadpole improved with unimproved data (left), and $z = 0$ with $z = 1$ (right).

significant. Also, the mass dependence of the $\mathcal{O}(a)$-improved vector current is not known at tree level, as mentioned previously.

Using the two lightest quark masses, $Z_V(m = 0)$ is found to be 0.932 for the tadpole improved action with z=1. This agrees poorly with the perturbative value [26] of 0.99, but the ratio $Z_V^{z=0}/Z_V^{z=1}$ is in good agreement with perturbation

β	κ	m_{PS}^2	Z_A^L	Z_P/Z_S
6.2	0.14262	0.208	$1.040\ ^{+\ 10}_{-\ 9}$	$0.693\ ^{+\ 28}_{-\ 40}$
	0.14144	0.663	$1.047\ ^{+\ 8}_{-\ 8}$	$0.649\ ^{+\ 9}_{-\ 8}$
6.0	0.1432	0.615	$1.097\ ^{+\ 19}_{-\ 17}$	$0.607\ ^{+\ 13}_{-\ 28}$

Table 3.5: Values of the renormalisation constants Z_A^L and Z_P/Z_S as functions of the quark mass.

theory.

The comparison of the data at $z = 0$ and $z = 1$ is inconclusive, but indicates that it is possible to use either prescription. A more recent and detailed study of these mass effects can be found in [27].

3.4 Axial current

The axial vector renormalisation constant Z_A^L is determined using eq. (2.135), with $\nu = \rho = i$ and summing over $i = 1, 2, 3$, using the values for Z_V^L quoted in table 3.2 as input. The results are obtained at β=6.2, using 60 configurations for κ=0.14144 and 26 configurations for κ=0.14262, and at β=6.0 using 36 configurations for κ=0.1432. The results are plotted against t in fig.3.8 for β=6.2, and in fig.3.9 for β=6.0. We see that, apart from the effect of the contact terms on the first few timeslices, they show virtually no dependence on t, especially for κ=0.14144. Since the Ward identities are time independent, this is to be expected. For the two other κ values, the data becomes unreliable at high t. The best estimates are obtained from fitting to timeslices 7–22 for κ=0.14144 and to timeslices 6–16 for κ=0.14262 and 0.1432. The results are given in table 3.5.

Within the statistical errors, these results show no dependence of Z_A on the quark mass. This is confirmed by simulations at β=6.0 [28]. The comparison with results from perturbation theory is more interesting: one-loop calculations with a mean-field rescaled coupling constant give $Z_A \approx 0.97$, which is considerably lower than

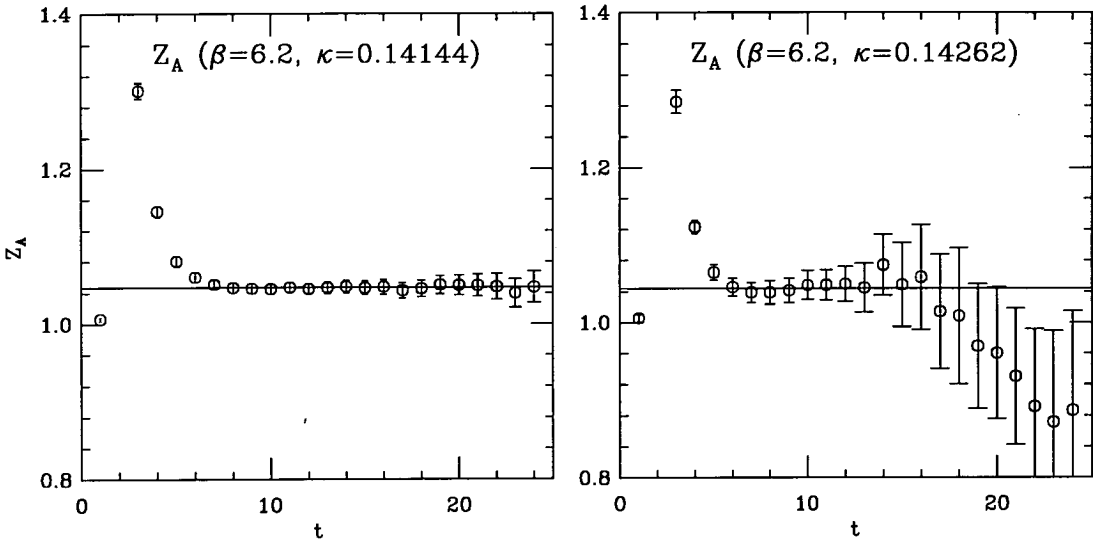

Figure 3.8: Z_A^L as a function of t for $\kappa = 0.14144$ (left) and $\kappa = 0.14262$ (right).

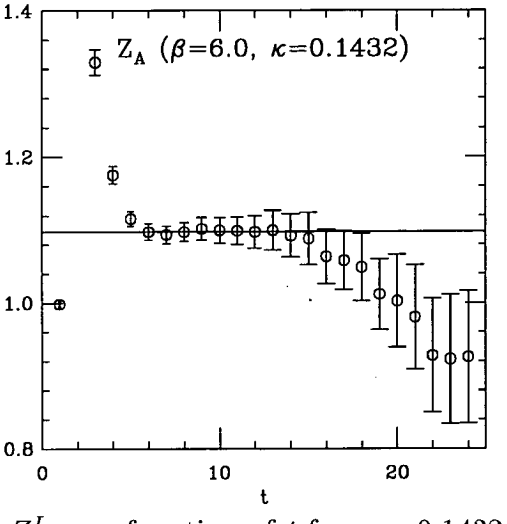

Figure 3.9: Z_A^L as a function of t for $\kappa = 0.1432, \beta = 6.0$

these non-perturbative results. The discrepancy is higher at lower β, as expected, and the value for β=6.0 is consistent with the value of 1.09 quoted in [21] (and within 2σ of the updated value [29] of 1.06(2)).

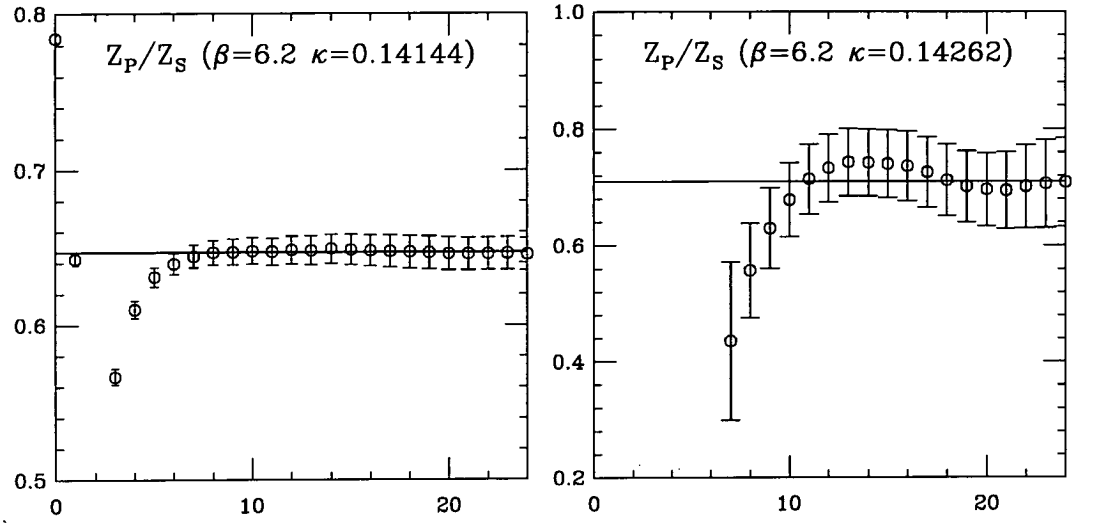

Figure 3.10: Z_P/Z_S as a function of t for $\kappa = 0.14144$ (left) and $\kappa = 0.14262$ (right).

3.5 Pseudoscalar and scalar densities

The ratio of pseudoscalar to scalar renormalisation constant is determined from (2.136), using the same ensembles as for Z_A. Z_P/Z_S is plotted as a function of t in figs.3.10 and 3.11. For β=6.2, κ=0.14144 a fit to timeslices 7–24 was used, while for κ=0.14262 the fit was to timeslices 16–24, and at β=6.0, κ=0.1432, a fit range of 8–20 was used. The best estimates are given in table 3.5. The uncertainty in these results is too large to determine whether there is any dependence on the quark mass. Perturbative calculations with a mean-field rescaled coupling constant give Z_P/Z_S=0.70. As can be seen, the result for the heavier quark mass (which is the more accurate) is slightly lower than this, while the lighter quark mass gives a value compatible with perturbative results (although the errors here are still quite large). At β=6.0, the perturbative estimate is Z_P/Z_S=0.68, confirming that, as in the case with Z_A, the discrepancy decreases with increasing β.

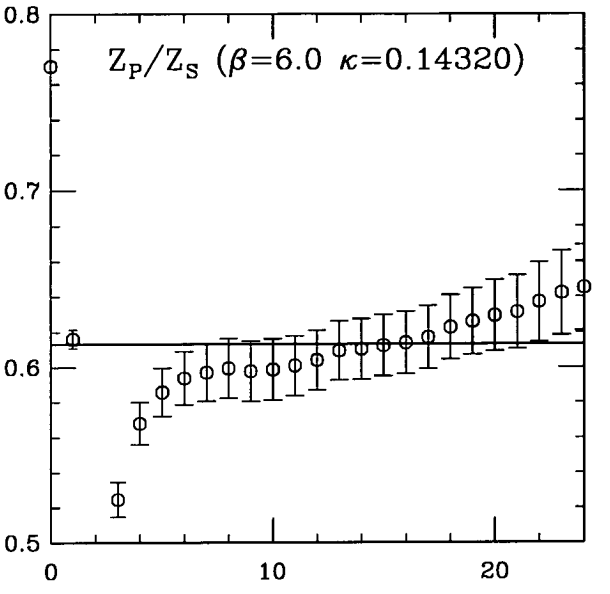

Figure 3.11: Z_P/Z_S as a function of t for $\kappa = 0.1432, \beta = 6.0$

3.6 Effect on decay constants

Table 3.6 shows how the values for the decay constants reported in [30], for β=6.2, change when we use the results given above for the renormalisation constants. For Z_V, the values in table 3.2 have been extrapolated to the limit of zero quark mass, giving $Z_V = 0.817(2)$. When determining f_{K^*} and f_ϕ, an additional uncertainty, due to the quark mass dependence, of ± 0.008, is added, corresponding to the difference between the values at the largest quark mass and in the chiral limit. For Z_A, a best estimate is obtained by combining the results at the two κ-values, of $Z_A = 1.045\ ^{+\ 10}_{-\ 14}$, with the errors corresponding to the spread between the highest and lowest estimate. We see that all the decay constants move closer to the experimental values, but that a significant discrepancy still remains, especially for f_ϕ and f_K. This may be partly related to uncertainties in the determination of κ_s. f_π turns out to be about 3σ away from its experimental value. The APE collaboration has found $f_\pi/(m_\rho Z_A) = 0.186(20)$ at $\beta = 6.2$ [32], which gives a value for f_π/m_ρ compatible with experiment. Recently obtained results with a

	old estimates	updated estimates	experiment
f_π	$102 \begin{smallmatrix}+6\\-7\end{smallmatrix}$ MeV	$110 \begin{smallmatrix}+7\\-8\end{smallmatrix}$ MeV	132 MeV
f_K	$123 \begin{smallmatrix}+5\\-6\end{smallmatrix}$ MeV	$133 \begin{smallmatrix}+7\\-7\end{smallmatrix}$ MeV	160 MeV
$1/f_\rho$	$0.316 \begin{smallmatrix}+7\\-13\end{smallmatrix}$	$0.311 \begin{smallmatrix}+7\\-13\end{smallmatrix}$	0.28
$1/f_{K^*}$	$0.298 \begin{smallmatrix}+5\\-9\end{smallmatrix}$	$0.293 \begin{smallmatrix}+5+1\\-9-1\end{smallmatrix}$	
$1/f_\phi$	$0.280 \begin{smallmatrix}+3\\-6\end{smallmatrix}$	$0.276 \begin{smallmatrix}+3+1\\-6-1\end{smallmatrix}$	0.23
f_π/m_ρ	$0.138 \begin{smallmatrix}+6\\-9\end{smallmatrix}$	$0.149 \begin{smallmatrix}+6\\-10\end{smallmatrix}$	0.172
f_K/m_ρ	$0.160 \begin{smallmatrix}+7\\-8\end{smallmatrix}$	$0.172 \begin{smallmatrix}+8\\-9\end{smallmatrix}$	0.208
f_K/m_{K^*}	$0.144 \begin{smallmatrix}+4\\-6\end{smallmatrix}$	$0.155 \begin{smallmatrix}+5\\-7\end{smallmatrix}$	0.179

Table 3.6: Values of decay constants in physical units, using perturbative and non-perturbative values for the renormalisation constants. The second set of errors in the vector meson decay constants are systematic uncertainties due to the quark mass dependence of Z_V.

tadpole improved action [31] give $f_\pi/(Z_A m_\rho)$=$0.162 \begin{smallmatrix}+5\\-4\end{smallmatrix}$. Using the perturbative value for Z_A, which for the tadpole improved action is 0.93 at $\beta = 6.2$, this still gives a value for f_π/m_ρ of $0.151 \begin{smallmatrix}+5\\-4\end{smallmatrix}$ which is 4σ lower than the experimental value. It is possible that a non-perturbative determination of Z_A will improve on this, although it is again unlikely that it will bridge the gap between the lattice estimate and experiment.

All the work reported in this chapter was performed two years or more ago. Since then, there have been a number of new developments, both theoretically and in algorithms and computer power. This means that the results reported here are to a large extent already out of date, and must be updated with new results for the new actions that are now being used.

Chapter 4

The quark–gluon vertex

4.1 Continuum symmetries and form factors

The continuum vertex function (fig. 4.1) can be derived from the effective action Γ, cf. eq. (1.10)

$$\Lambda^a_\mu(x,y,z)^{ij}_{\alpha\beta} = \frac{\delta^3\Gamma}{\delta\psi^i_\alpha(x)\delta A^a_\mu(y)\delta\overline{\psi}^i\beta(z)} \tag{4.150}$$

and the momentum-space vertex is defined by

$$(2\pi)^4\delta^4(p+q-r)\Lambda^a_\mu(p,q) = \int d^4x d^4y d^4z e^{-i(px+qy-rz)}\Lambda^a_\mu(x,y,z) \tag{4.151}$$

The only possible dependence this can have on the group coordinates a,i,j is proportional to T^a_{ij}. We can therefore consider only $\Lambda_\mu(p,q)$, defined by

$$(\Lambda^a_\mu)^{ij}_{\alpha\beta} = T^a_{ij}(\Lambda_\mu)_{\alpha\beta} \tag{4.152}$$

Lorentz invariance and parity conservation require that this takes the form

$$\begin{aligned}\Lambda_\mu(p^2,q^2,pq) = {} & F_1 p_\mu + F_2 q_\mu + F_3\gamma_\mu \\ & + F_4\ \not{p}p_\mu + F_5\ \not{p}q_\mu + F_6\ \not{q}p_\mu + F_7\ \not{q}q_\mu\end{aligned} \tag{4.153}$$

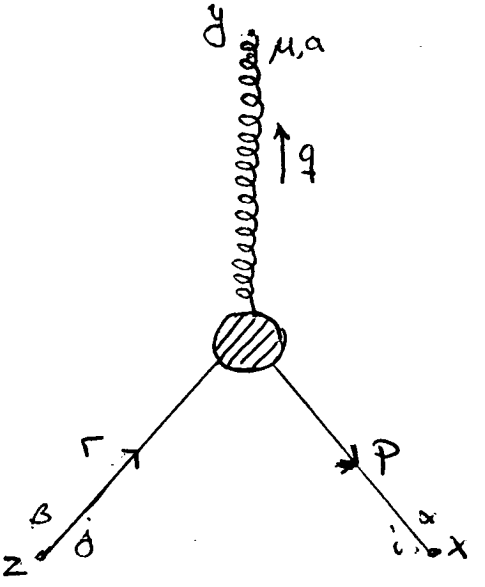

Figure 4.1: The quark–gluon vertex.

$$+F_8\sigma_{\mu\nu}p^\nu + F_9\sigma_{\mu\nu}q^\nu$$

where all the F's depend only on the invariants p^2, q^2 and pq.

At tree level, this reduces to $\Lambda^0_\mu = ig_0\gamma_\mu$. From this we can see that the form factor containing the running coupling is F_3, while all the other form factors are expected to be finite.

4.2 Method for extracting the renormalised coupling

4.2.1 Definitions and principles

We define the lattice gluon field $A_\mu(x)$, which in the continuum limit becomes $aA_\mu^{cont}(x)$, as

$$A_\mu(x) = \frac{1}{2ig_0}\left(U_\mu(x) - U_\mu^\dagger(x)\right) - \frac{1}{6ig_0}\mathrm{Tr}\left(U_\mu(x) - U_\mu^\dagger(x)\right) \tag{4.154}$$

The momentum-space gluon field then becomes[1]

$$\begin{aligned} A_\mu(q) &= \sum_x e^{-iqx} A_\mu(x) \\ &= \frac{1}{2ig_0}\left(U_\mu(q) - U_\mu^\dagger(-q)\right) - \frac{1}{6ig_0}\mathrm{Tr}\left(U_\mu(q) - U_\mu^\dagger(-q)\right) \end{aligned} \tag{4.155}$$

The Lie algebra-valued gluon fields can be computed by tracing with the Gell-Mann matrices

$$\mathrm{Tr}\lambda^a A_\mu = \mathrm{Tr}\lambda^a \sum_b \frac{\lambda^b}{2} A_\mu^b = \sum_b \delta^{ab} A_\mu^b = A_\mu^a \tag{4.156}$$

We can define the configuration space quark–gluon vertex function as

$$V_\mu^a(x,y,z)_{\alpha\beta}^{ij} = \left\langle \psi_\alpha^i(x)\overline{\psi}_\beta^j(z)A_\mu^a(y)\right\rangle = \left\langle S_{\alpha\beta}^{ij}(x,z)A_\mu^a(y)\right\rangle \tag{4.157}$$

Fourier transforming this and invoking translational invariance gives us the full

[1] This should really be $A_\mu(q) = \sum_x e^{-iq(x+\hat{\mu}/2)}A_\mu(x)$, but we are keeping $q_\mu = 0$, so it makes no difference.

(unamputated) momentum space vertex function:

$$\begin{aligned}
&\sum_{x,y,z} e^{-i(px+qy-rz)} \left\langle \psi^i_\alpha(x) A^a_\mu(y) \overline{\psi}^j_\beta(z) \right\rangle \\
&= \sum_z e^{-i(p+q-r)z} \sum_{x,y} e^{-i(p(x-z)+q(y-z))} \left\langle \psi^i_\alpha(x-z) A^a_\mu(y-z) \overline{\psi}^j_\beta(0) \right\rangle \\
&= \sum_z e^{-i(p+q-r)z} \sum_{x,y} e^{-i(px+qy)} \left\langle \psi^i_\alpha(x) A^a_\mu(y) \overline{\psi}^j_\beta(0) \right\rangle \\
&= V\delta(p+q-r) \left\langle S^{ij}_{\alpha\beta}(p) A^a_\mu(q) \right\rangle \\
&= V\delta(p+q-r)\, G^a_\mu(p,q)^{ij}_{\alpha\beta}
\end{aligned} \tag{4.158}$$

and the proper vertex function

$$\Lambda^{a,\mathrm{lat}}_\mu(p,q) = \langle S(p+q)\rangle^{-1} \left\langle S(p) A^a_\mu(q) \right\rangle \langle S(p)\rangle^{-1} \langle D(q)\rangle^{-1} \tag{4.159}$$

where the momentum-space quark propagator $S(p)$ is

$$S(p) = \sum_x e^{-ipx} S(x,0) \tag{4.160}$$

$D(q)$ is the gluon propagator,

$$D^{ab}_{\mu\nu}(q) = \delta^{ab} P_{\mu\nu}(q) D(q) \tag{4.161}$$

and the projector $P_{\mu\nu}(q)$ is

$$P_{\mu\nu}(q) = \delta_{\mu\nu} - (1-\xi)\frac{q_\mu q_\nu}{q^2} \tag{4.162}$$

In the Landau gauge (ξ=0), $P_{\mu\nu}$ becomes the transverse projector $T_{\mu\nu}$, and $D(q)$ can be determined by

$$D(q) = \frac{1}{3(N_C^2-1)} \sum_{\mu,a} D^{aa}_{\mu\mu}(q) \tag{4.163}$$

At tree level, this becomes

$$\Lambda_\mu^{a(0)}(p,q) = -ig_0 T^a T_{\mu\nu}(q)\left(\gamma_\nu \cos\frac{(2p+q)_\nu}{2} - i\sin\frac{(2p+q)_\nu}{2}\right) \tag{4.164}$$

We will also define the colour-traced full vertex function

$$G_\mu(p,q)_{\alpha\beta} = \frac{2}{N_C^2-1}\sum_{ij,a} T_{ij}^a G_\mu^a(p,q)_{\alpha\beta}^{ji} \tag{4.165}$$

F_3 may be extracted by exploiting the symmetries of the problem. First, we isolate F_3 and F_4

$$\mathrm{Tr}\gamma_\mu \Lambda_\mu(p, q=0) = 4F_3(p^2) + 4p_\mu^2 F_4(p^2) \tag{4.166}$$

where no sum over μ is implied. We can then eliminate F_4 by imposing an appropriate kinematics, e.g. $p_\mu = 0, p_\nu \neq 0$ with $\mu \neq \nu$.

Finally, we define the renormalised coupling as

$$g_R(p^2) = iZ_2(p)Z_3^{1/2}(p)F_3(p^2) \tag{4.167}$$

where Z_2 and Z_3 are the renormalisation constants for the quark and gluon fields. Z_2 may be determined from (2.140), while Z_3 is defined by

$$D_{\mu\nu}(q^2)|_{q^2=p^2} = T_{\mu\nu}(p)Z_3(p)\frac{1}{p^2} \tag{4.168}$$

From this, we can compute $g_R(q^2)$, which should be independent of the bare coupling $g_0^2 = 6/\beta$, and relate this to the running coupling calculated in other schemes, eg, $g_R^{\overline{MS}}(q^2)$ or the lattice 3-gluon coupling [33]. It is worth noting that, since this scheme is defined in the continuum as well as on the lattice, the matching with $g_R^{\overline{MS}}(q^2)$ can be performed entirely within continuum perturbation theory, provided there is a region where perturbation theory is valid and lattice artefacts are insignificant.

4.2.2 Computational details

All the results in this chapter have been obtained with the Wilson gauge action at $\beta = 6.0$ on a $16^3 \times 48$ lattice. The gauge fields were generated with a Hybrid Over-Relaxed algorithm, with configurations separated by 800 sweeps. The quark propagators have been generated using a tadpole improved SW fermion action, with $c_{SW} = 1.48$, for one value of $\kappa/u_0 = 0.1370$, which corresponds to a pseudoscalar mass of 830 MeV.

The gauge fields have been fixed to Landau gauge, using a Fourier accelerated algorithm [34] to deal with low-momentum modes. The Landau gauge condition has been achieved to an accuracy of

$$\frac{1}{VN_C}\sum_{x,\mu}|\partial_\mu A_\mu|^2 < 10^{-12} \tag{4.169}$$

It is necessary to be careful when Fourier transforming the quark propagators. Having chosen antiperiodic boundary conditions in the time direction, we have to choose half-integer values for the momenta in the time direction

$$p_t a = 2\pi(n_t + \frac{1}{2})/L_t \qquad n_t = 0, 1, \ldots, L_t - 1 \tag{4.170}$$

while the spatial momenta (and the gauge momenta in all directions) have integer values,

$$p_i a = 2\pi n_i/L_i \qquad n_i = 0, 1, \ldots, L_i - 1 \tag{4.171}$$

The time Fourier transformation for the quarks cannot be performed directly using a standard FFT routine; instead, $S(t)$ is extended onto a lattice of length $2L_t$, using $S(t + L_t) = -S(t)$, and picking only the odd momenta. Alternatively, and equivalently, we could perform a standard FFT on $\tilde{S}(t) = e^{-i\pi t/L_t}S(t)$.

The analysis is performed as in chapter 3, using least χ^2 fits and with the errors obtained from bootstrap samples. However, the large datasets involved give

problems. To circumvent these, the data have been divided into 4 batches of 83 configurations each, with 100 bootstrap samples generated for the average $\langle K_\mu \rangle = i\mathrm{Tr}\gamma_\mu \Lambda_\mu(p,q)$ and the covariance matrix $\langle K_\mu(\vec{p},p_t;q)K_\mu(\vec{p},p_t';q)\rangle$ (so that the correlation between K_μ for different p_t can be taken into account) for each batch, with different seeds used for the random number generator for each batch. A combined estimate for K_μ and $K_\mu K_\mu'$ is then obtained from

$$K_\mu = \frac{1}{4}\sum_{i=1}^{4} K_\mu^i$$

for each bootstrap sample of K_μ, and similarly for the covariance matrix. This is a good estimate provided the average and covariance for each batch provide reasonable estimates.

4.3 Determination of Z_2 and Z_3

The quark field renormalisation constant Z_2 has been determined using equation (2.140). The results are plotted as a function of $|pa|$ in fig. 4.2. We see that Z_2 has large ambiguities. A natural assumption is that these ambiguities arise from violations of rotational symmetry, and this is confirmed by fig. 4.3, where it is plotted for momenta only in certain directions.

The main ambiguity is between on-axis and off-axis points, as we can see by comparing fig. 4.3 (a)–(c). The values for spatial on-axis points are lower than those which are on-axis in the time direction, because it is not possible to set $p_t = 0$. Comparing (c) and (d), we see there is also an ambiguity at high momenta, which accounts for the 'spurs', and is almost removed entirely by selecting only low-lying momentum values, as in (d).

These violations are primarily of $\mathcal{O}(pa)$, since the SW action is only $\mathcal{O}(a)$-improved for on-shell quantities. Following the prescription of [17], one could 'rotate' the

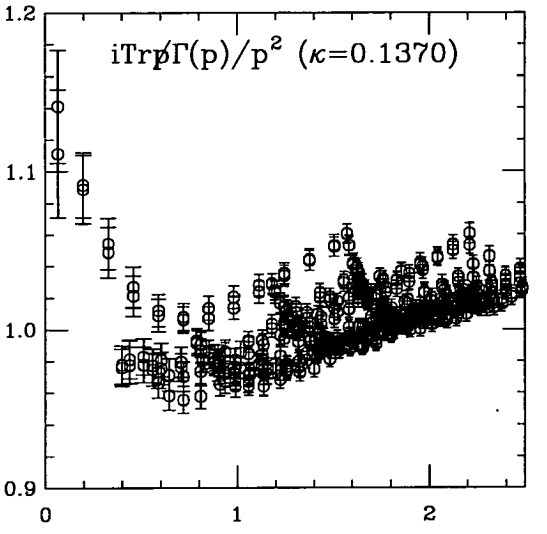

Figure 4.2: Z_2 as a function of $|pa|$, for 80 configurations

propagators at either end with $(1 + \frac{1}{4}(\not{D} + m_0))$ (cf. sections 2.3.1 and 3.3.2), and there are indications that this would help. An earlier study, using the same (rotated) propagators as were used at $\beta = 6.0$ in section 3.3, had no ambiguity between on-axis and off-axis points, but still large high-momentum ambiguities, as figure 4.4 shows. However, attempts to add these rotations by hand by replacing $\not{D}$ with $\not{p}$ have not been successful.

Z_2 has been fitted to a phenomenological curve (to be used as input when computing the renormalised coupling), $Z_2 = c_0 + c_1 \ln(pa) + c_2(pa)^2$, using only the on-axis points in the time direction. The best estimates for the parameters are given in table 4.1.

c_0	$0.960 \begin{smallmatrix} + 8 \\ - 9 \end{smallmatrix}$
c_1	$-0.065 \begin{smallmatrix} + 9 \\ - 14 \end{smallmatrix}$
c_2	$0.054 \begin{smallmatrix} + 7 \\ - 6 \end{smallmatrix}$

Table 4.1: Parameters for the quark field renormalisation constant Z_2, from 83 configurations, 100 bootstrap samples.

The gluon field renormalisation constant Z_3 has been determined from (4.168), and is shown as a function of qa in figure 4.5. This has been fitted to a phenomenological curve $Z_3(qa) = A_0 + A_1 \ln(qa) + A_2(qa)^2$ for $0.45 < qa < 1.57$, and to a

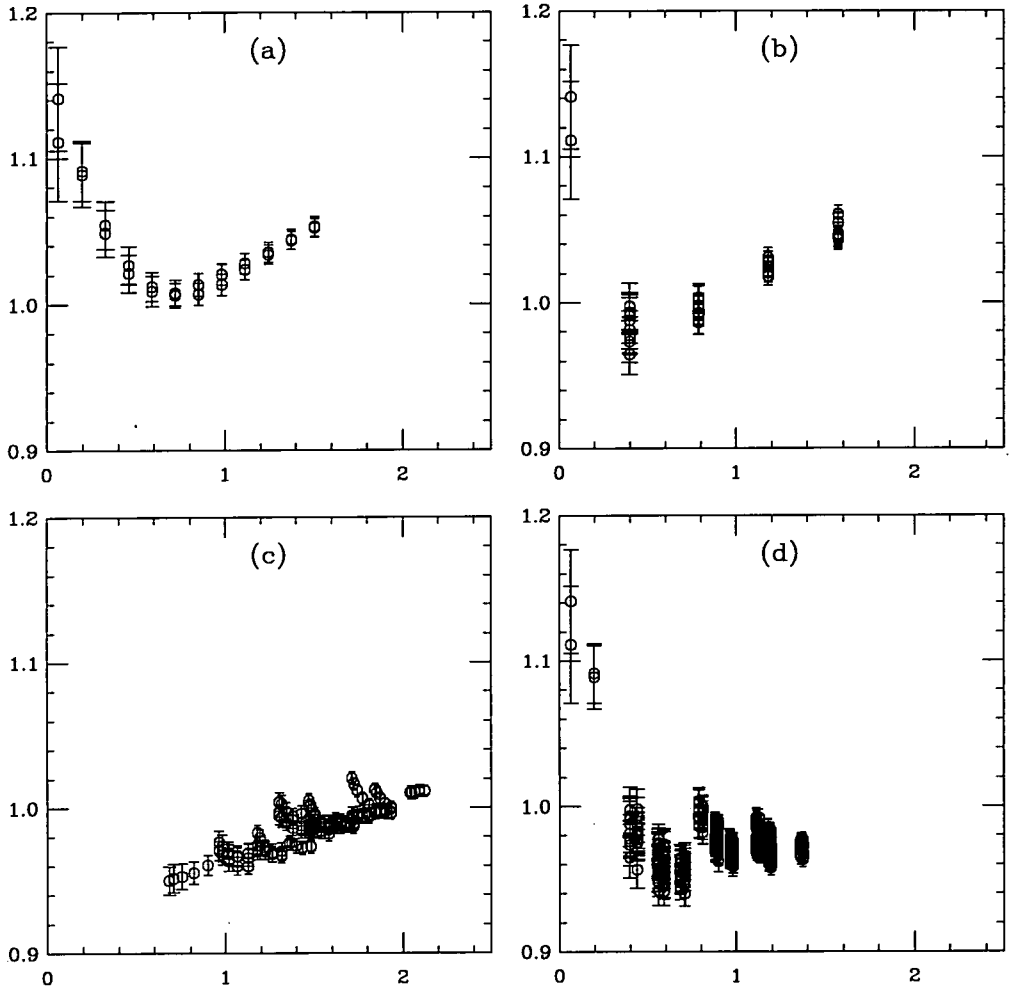

Figure 4.3: Z_2 as a function of $|pa|$, for 80 configurations, selected momenta. (a) Momenta only in the time direction; (b) momenta on-axis in spatial directions, with $n_t = \pm\frac{1}{2}$; (c) off-axis momenta only; (d) $|n_i| \leq 2$; $|n_t| \leq \frac{5}{2}$

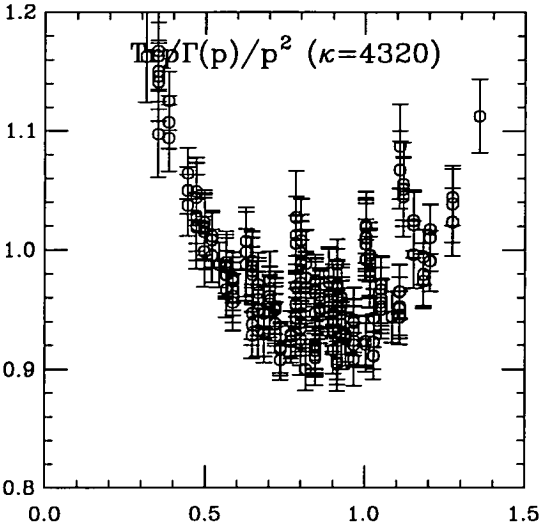

Figure 4.4: Z_2 as a function of $|pa|$, for 8 configurations, using rotated propagators, $c_{SW} = 1, \kappa = 0.1432$

curve $Z_3(qa) = a_1(qa) + a_2(qa)^2 + a_3(qa)^3$ for $qa < 0.45$. The best estimates for the parameters are given in table 4.2. A high accuracy is obtained already for 20 configurations, and only minimal violations of rotational symmetry are observed.

$pa < 0.45$		$pa > 0.45$	
a_1	$6.0\ ^{+1.4}_{-0.9}$	A_0	$2.12\ ^{+\ 2}_{-\ 3}$
a_2	$38\ ^{+\ 6}_{-\ 9}$	A_1	$-2.25\ ^{+\ 6}_{-\ 8}$
a_3	$-70\ ^{+\ 13}_{-\ 9}$	A_2	$0.347\ ^{+\ 25}_{-\ 20}$

Table 4.2: Parameters for the gluon renormalisation constant Z_3, from 20 configurations, 100 bootstrap samples.

It should be emphasised that these fits are only performed to facilitate the computation of the running coupling $g_R(p)$, and no physical significance should be attached to the phenomenological parameters quoted.

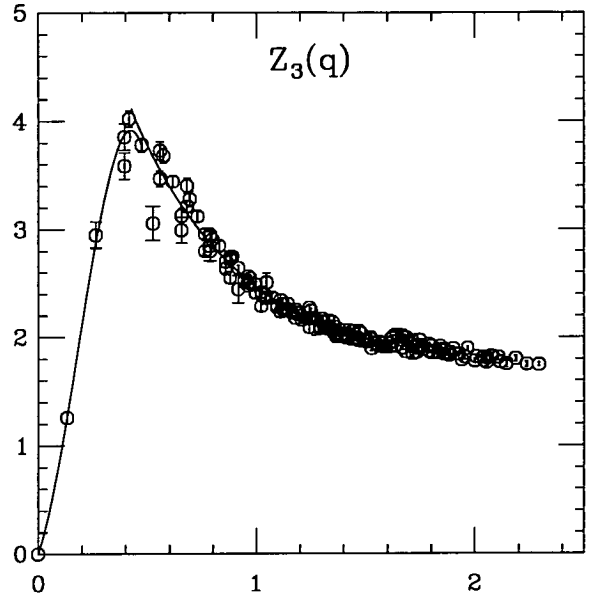

Figure 4.5: Z_3 as a function of $|qa|$, for 20 configurations

4.4 The F_3 form factor and the running coupling

4.4.1 The unamputated vertex

$\mathrm{Tr}\gamma_\mu G_\mu(p,q)$ is shown as a function of $p = (0,0,0,p_t)$ for $q = 0$ (with $\mu = 1$) in fig. 4.6. We see that there is a clean signal which falls off smoothly with p.

Fig. 4.7 shows $i\mathrm{Tr}\gamma_1 G_1$ for $n_{q_y} = 1$ and 2. For $n = 1$ there is still a clear signal, although the amplitude has fallen off from $q = 0$ to $qa = \pi/8$ as it does from $p_t \sim 0$ to $p_t a \sim \pi/8$. However, for $n_q = 2$, as fig. 4.7 (b) shows, noise dominates, and insofar as there is a signal, it is negative. This indicates that a renormalisation scheme where F_3 is calculated as a function of q^2, keeping p=0, is not feasible.

Fig. 4.8 shows $i\mathrm{Tr}\gamma_1 G_1(p,q)$ for various non-zero p and q. The most interesting of these are (a) and (b), which show what happens to $\mathrm{Tr}\gamma_\mu G_\mu(p,q)$ when $p_\mu \neq 0$ or $q_\mu \neq 0$. Fig. 4.8 (a) shows that the signal is strongly suppressed when $q_\mu \neq 0$, and (b) indicates a highly non-trivial behaviour for $p_\mu \neq 0$. This indicates how the form factors for the proper vertex F_4–F_7 in (4.153) come into play for these

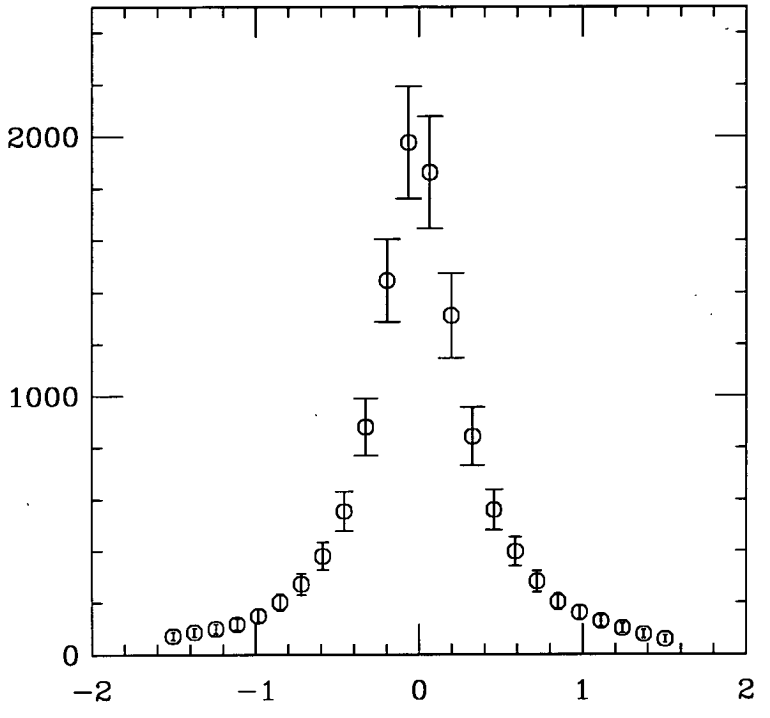

Figure 4.6: $\mathrm{Tr}\gamma^1 G_1(p,q)$ for $q = 0$, $p = (0, p_t)$, as a function of $p_t a$, for 83 configurations.

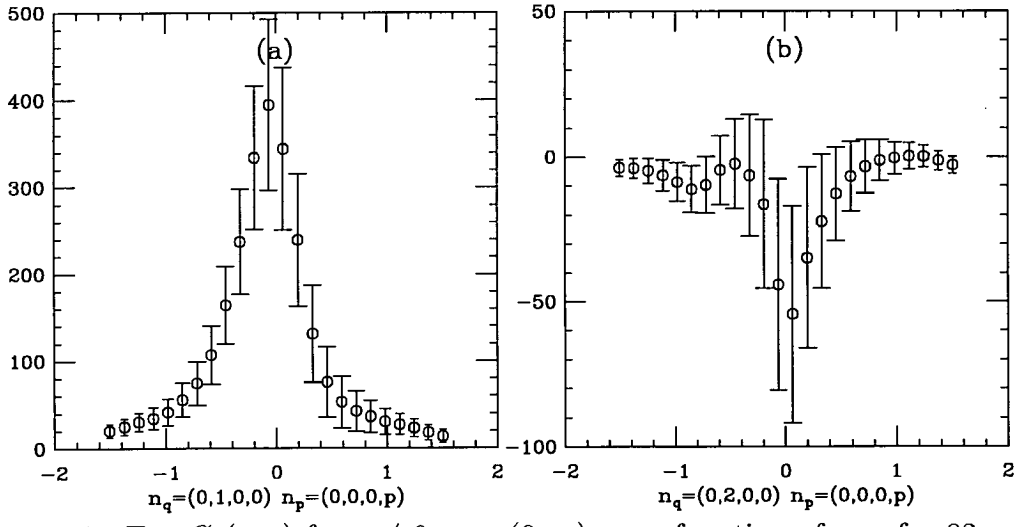

Figure 4.7: $\mathrm{Tr}\gamma_1 G_1(p,q)$ for $q \neq 0$, $p = (0, p_t)$, as a function of $p_t a$, for 83 configurations.

kinematics, something which is also manifest in the full vertex.

Fig. 4.8 (c) and (d) show that there is hardly any deterioration in the signal as p is increased in a perpendicular direction. As expected, the amplitude falls off with p. As (e) and (f) show, there is also a clear signal for $q_t \neq 0$, although we here see a more erratic behaviour for $p_t \sim 0$, as one would expect from fig. 4.7.

4.4.2 The proper vertex

The proper vertex has been computed as a function of p_t for different values of $\vec{p}, q$ in batches of 83 configurations, as described in section 4.2.2. Fig. 4.9 shows the vertex for $q = 0, \vec{p} = 0$ for each of the 4 batches, and for the combined estimate. It is evident that the data are distorted by large correlations, which are only evened out by the large number of configurations in the total ensemble. It also confirms that the sample size in each batch is large enough (at least for these momenta) to give a sufficiently reliable estimate of the vertex to justify the method used. But the spread between the data for different batches indicates that using much smaller samples could invalidate the assumptions the method is based on.

In this exploratory work, one component Λ_1 of the proper vertex has been chosen for detailed study. Rotational invariance would imply that the only thing we lose by this is statistics, since the other components are expected to behave in the same fashion. This is true within errors, as figure 4.10 shows. We have already seen in section 4.4.1 that additional form factors complicate the picture of $\mathrm{Tr}\gamma_\mu G_\mu$, and therefore also $K_\mu(p,q)$, when $p_\mu \neq 0$. This means that we should not expect K_4 to behave similarly to the other three components, since $p_4 = p_t$ is necessarily non-zero. Fig. 4.11 confirms this — indeed, apart from p_t close to zero, no signal can be observed.

One would expect that K_μ is symmetric in $p \to -p$ and $q \to -q$, at least when p and q are perpendicular, and $p_\mu = q_\mu = 0$. Fig. 4.12 shows that some violations

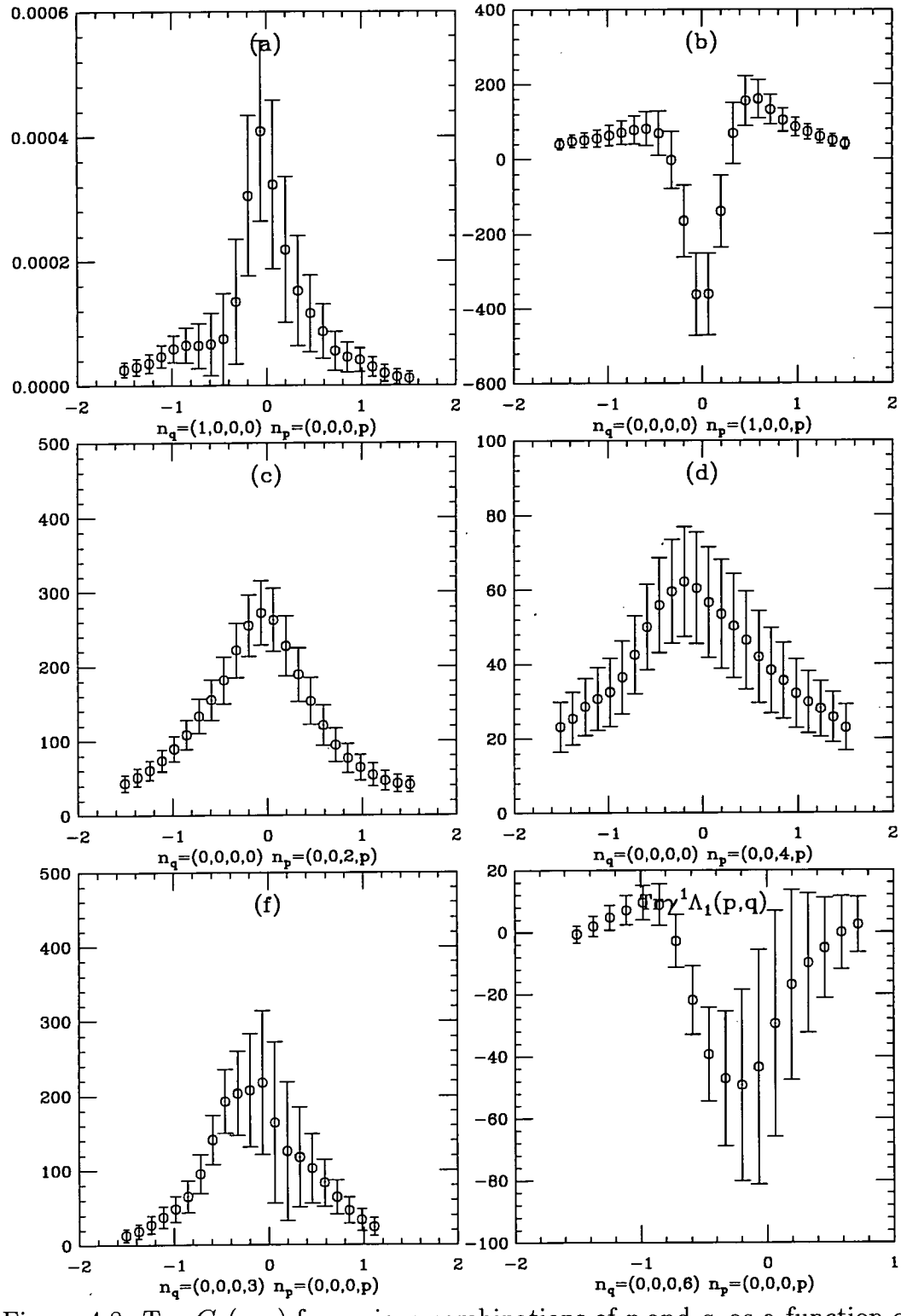

Figure 4.8: $\mathrm{Tr}\gamma_1 G_1(p,q)$ for various combinations of p and q, as a function of p_t.

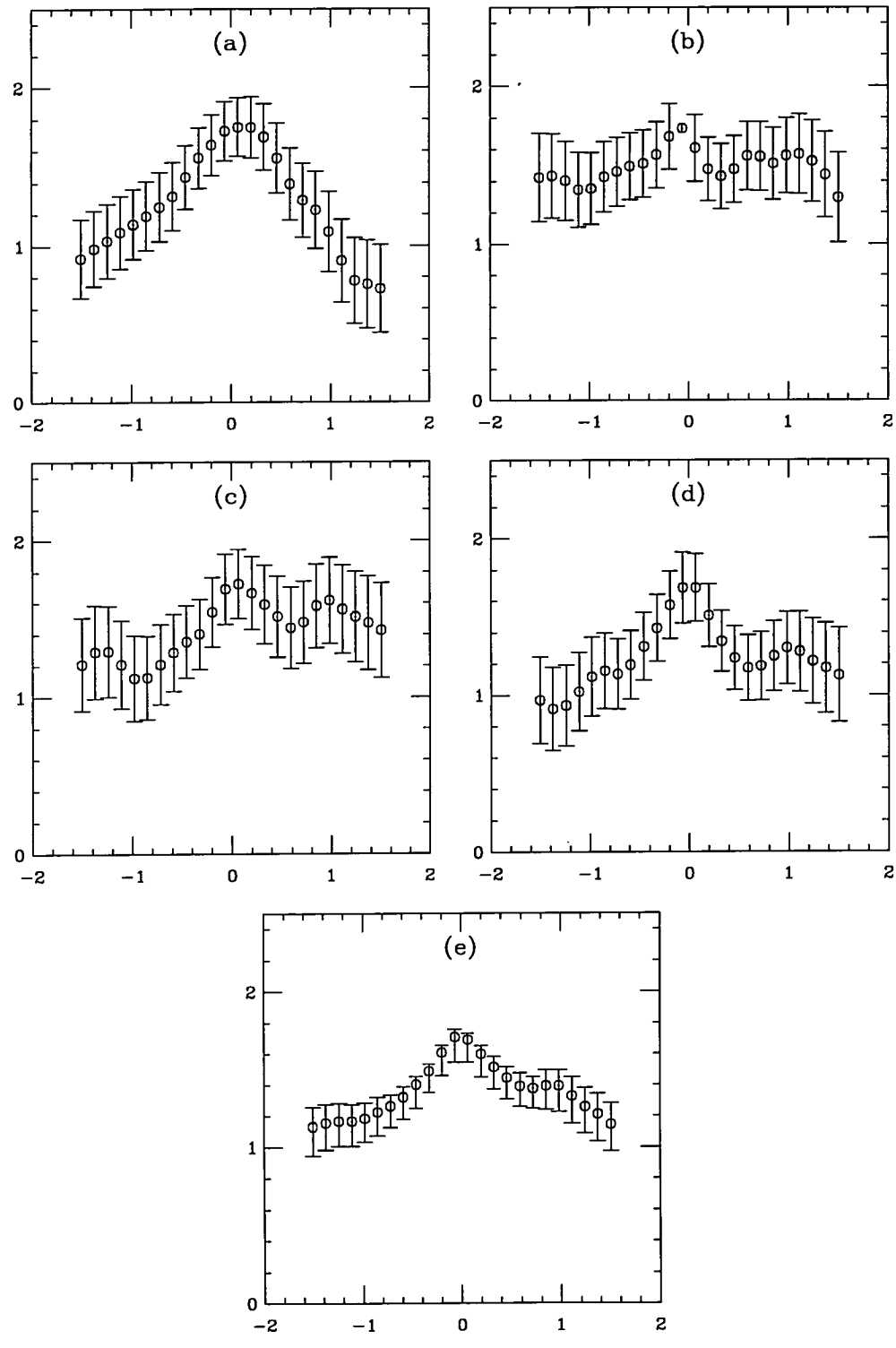

Figure 4.9: $K_1(p,q)$ for $q = 0$, $p = (0, p_t)$, as a function of $p_t a$, for 83 configurations (a)–(d), and for all 332 configurations (e).

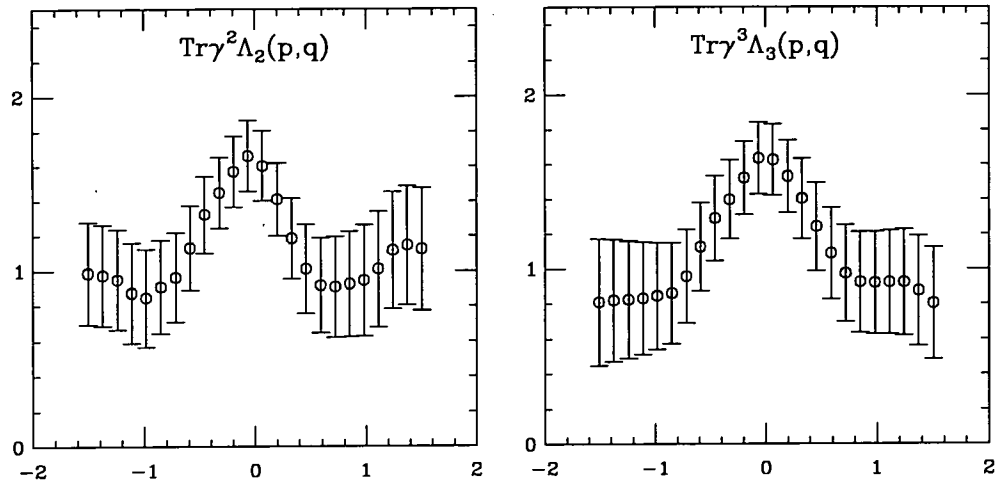

Figure 4.10: $K_2(p,q)$ and $K_3(p,q)$ for $q = 0$, $p = (0, p_t)$, as a function of $p_t a$, for 83 configurations.

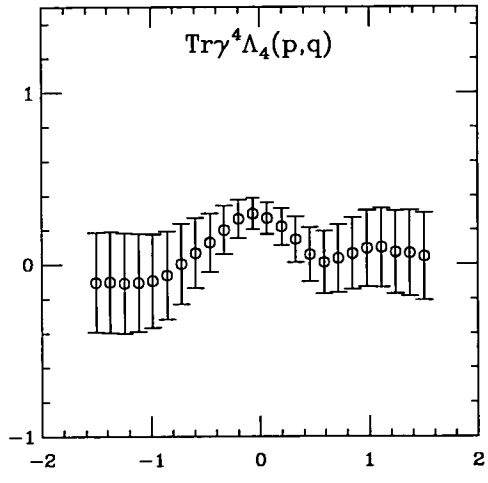

Figure 4.11: $K_4(p,q)$ for $q = 0$, $p = (0, p_t)$, as a function of $p_t a$, for 83 configurations.

of reflection symmetry may be present, but they are all within a few standard deviations. It should be emphasised that these are the only values of the momenta for which any significant violation of reflection symmetry can be detected. When computing the running coupling and Λ_{QCD}, all equivalent momenta have been averaged.

In fig. 4.13 K_1 is shown as a function of $|pa|$ for $q = 0$. This is equal to the form factor F_3, and as the figures show, it is a well-defined function of p (within the statistical errors) at least for $pa < 1 - 1.2$. Fig. 4.14 shows K_1 for $n_{q_y} = 1$. This shows a similar dependence on p as $F_3(p)$, although the errors are larger, as one would expect.

Fig. 4.15 shows $K_1(q_y a = \pi/4)$ as a function of $|pa|$. Although any signal here is swamped by the noise, it is still possible to detect a p dependence similar to the dependence for $q = 0$ and $q = \pm 1$.

K_1 is also shown as a function of $p_t a$ for several values of $q_t \neq 0$ in fig. 4.16. Since p and q are parallel in this case, it is difficult to give a physical interpretation of this, but it can be noted that

- The signal is most distinct for $p_t = -q_t/2$. This indicates that the leading dependence of the vertex on p and q is as a function of $p + q/2$, as indicated by the tree level expression (4.164).
- There is a clear signal for all values of q_t. This means that it may be feasible to choose an alternative renormalisation scheme, using the symmetric point $q_\nu = -2p_\nu$. This has the added advantage that finite size effects should play no role, and it is also a fairly commonly used scheme in perturbation theory.

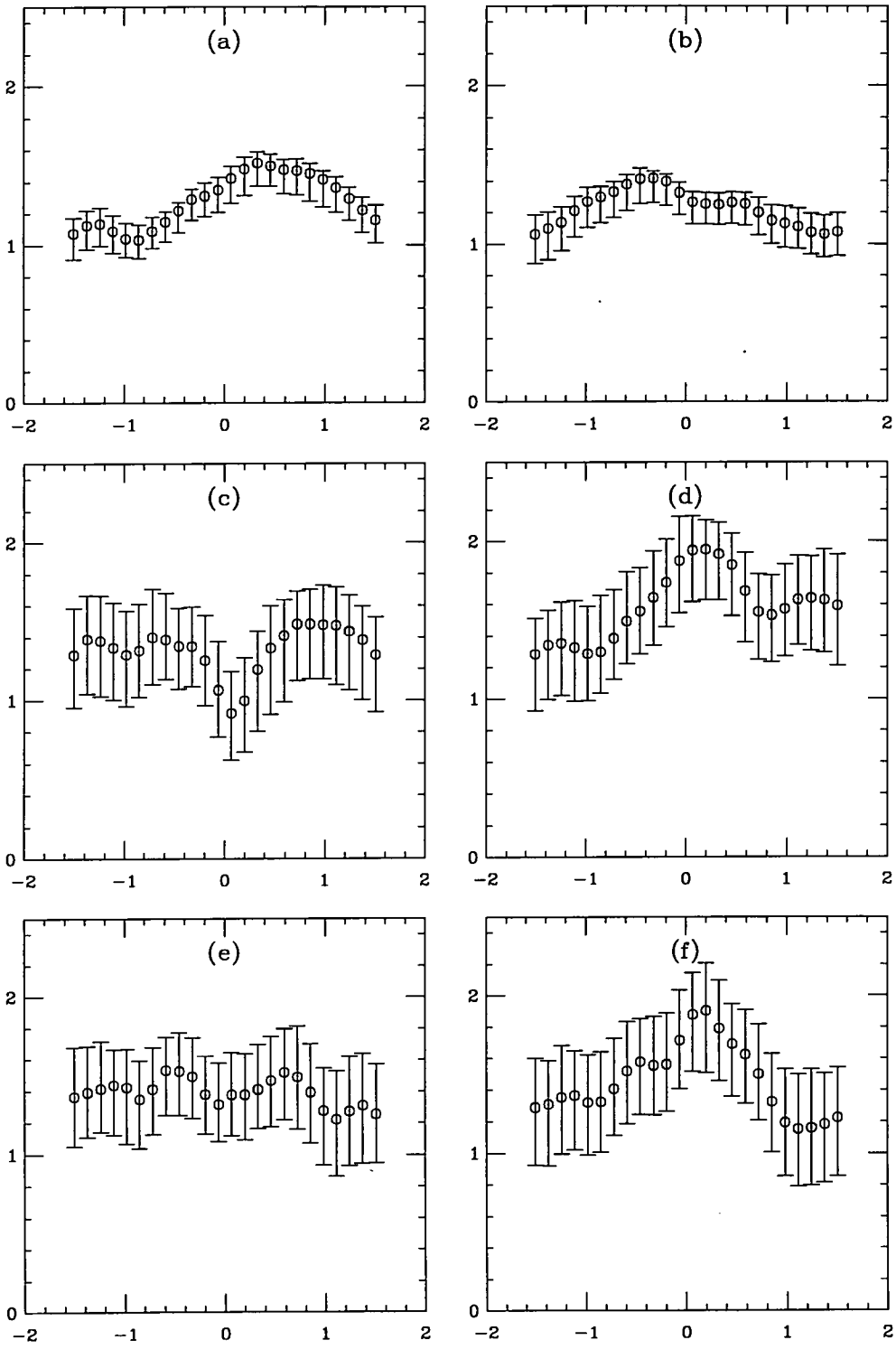

Figure 4.12: $K_1(p,q)$ for $q_y = \pm 1$, $p_z = \pm 1$, as a function of $p_t a$, for 332 configurations. (a) $q = 0, n_{p_z} = -1$ (b) $q = 0, n_{p_z} = 1$ (c) $n_{q_y} = 1, n_{p_z} = -1$ (d) $n_{q_y} = 1, n_{p_z} = 1$ (e) $n_{q_y} = -1, n_{p_z} = -1$ (f) $n_{q_y} = -1, n_{p_z} = 1$

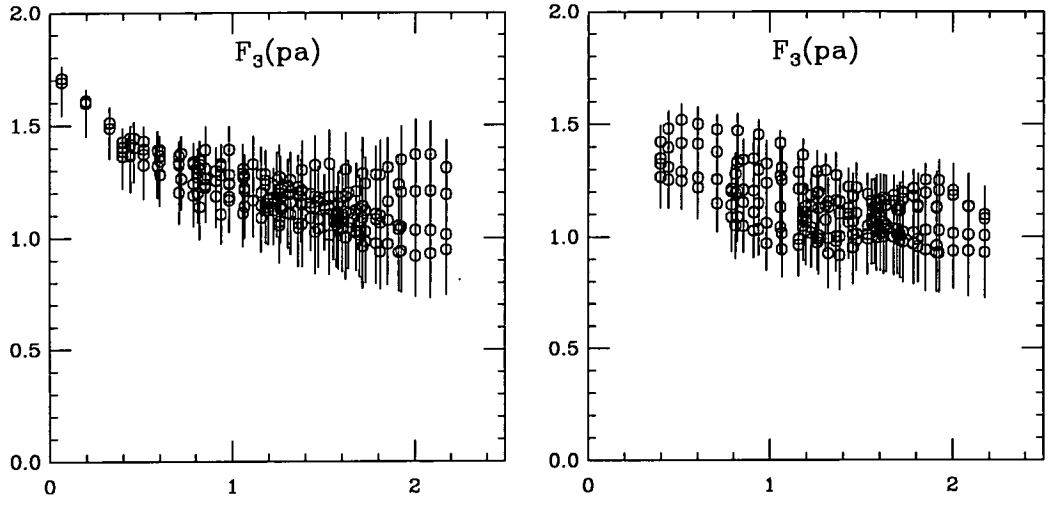

Figure 4.13: $F_3(p)$ as a function of $|pa|$ for $p = (0, p_y, 0, p_t)$ (left) and $p = (0, 0, p_z, p_t)$ (right).

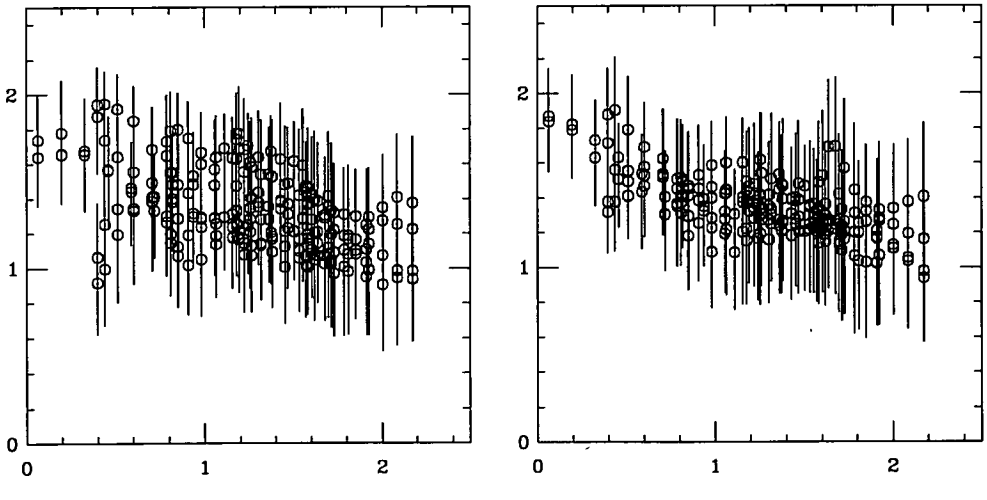

Figure 4.14: $K_1(p, q)$ as a function of $|pa|$ for $n_{q_y} = 1$ (left) and $n_{q_y} = -1$ (right).

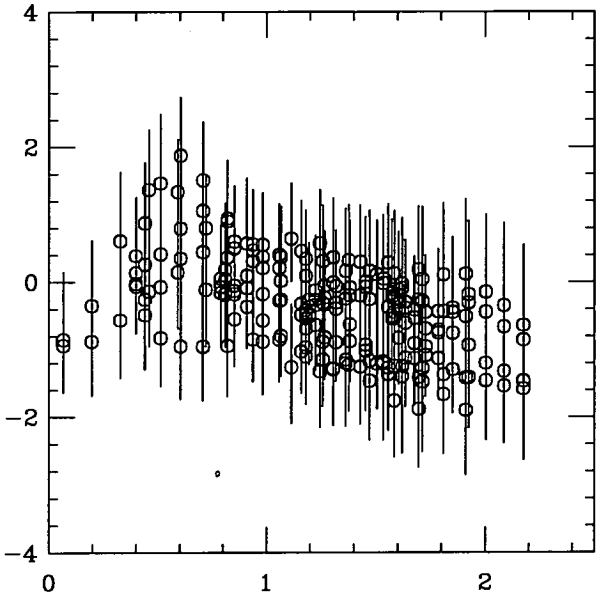

Figure 4.15: $K_1(p,q)$ as a function of $|pa|$ for $n_{q_y} = 2$

4.4.3 The running coupling and the Λ parameter

We see from fig. 4.13 that F_3 is a well-defined, decreasing function of p, although the uncertainties are still quite large. Fig. 4.17 shows F_3 for a restricted set of momenta ($p_\nu a \leq 1.2; |pa| \leq 1.5$), where equivalent momenta are averaged. This removes almost all the remaining ambiguities.

Using the values for Z_2 and Z_3 in 4.3, we obtain $g_R(p)$, which is shown in fig. 4.18. These results are close to those obtained from the 3-gluon vertex [33]. (The dip at low p is entirely due to the renormalisation factor Z_3.) We find that $\alpha_S(2\text{GeV}) = 0.27 \pm 0.06 \pm 0.03$, where the first error is statistical, and the second is the systematic error from the ambiguity in Z_2. The scale has been set to $a^{-1} = 2\text{GeV}$, from the string tension.

The QCD scale parameter Λ has been computed according to the 2-loop formula (2.111). The results are shown in fig. 4.19. It is difficult to draw any firm conclusions from this, since the data become very noisy at the point where 2-loop perturbation theory might become valid. However, it seems that Λ reaches a

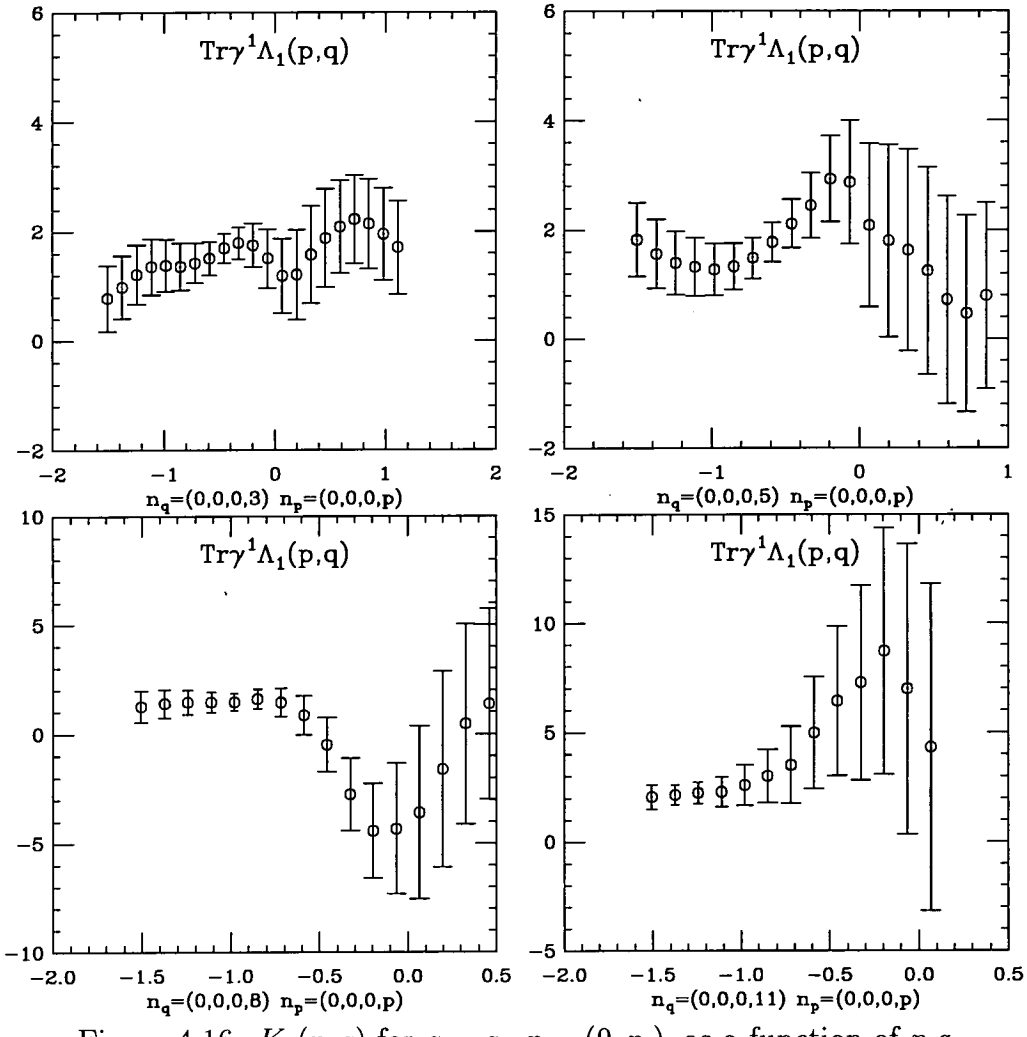

Figure 4.16: $K_1(p,q)$ for $q = q_t$, $p = (0, p_t)$, as a function of $p_t a$.

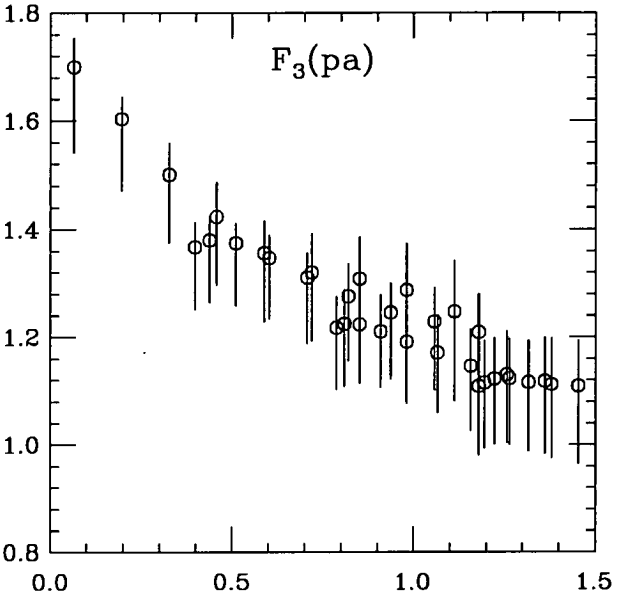

Figure 4.17: $F_3(p)$ as a function of p, with equivalent momenta averaged.

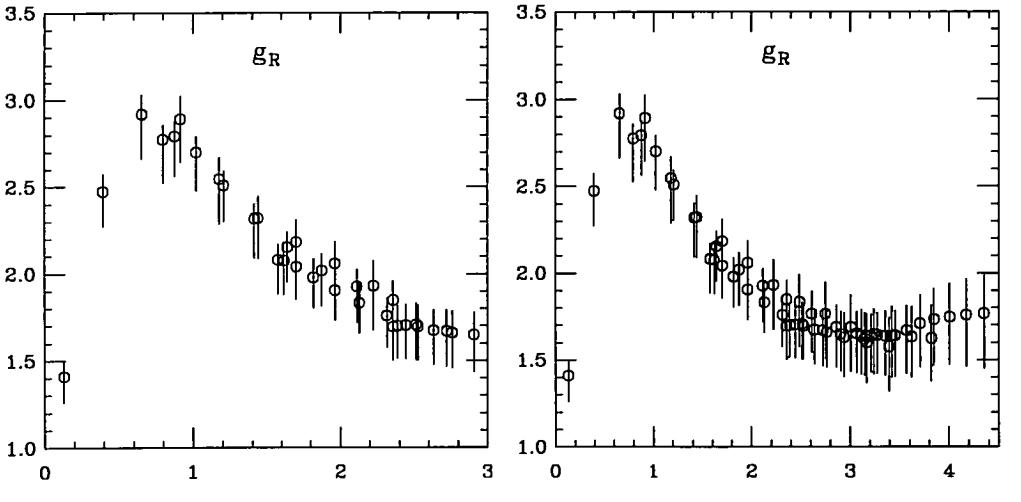

Figure 4.18: $g_R(p)$ as a function of p (GeV), for $p_\nu < 2.4$GeV (left), and for a wider range of momenta (right).

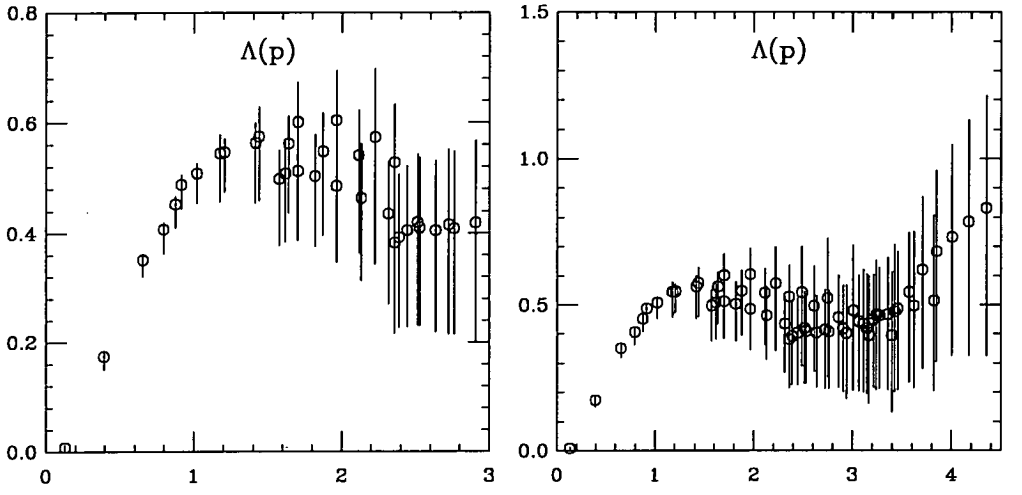

Figure 4.19: $\Lambda_{QCD}(p)$ (GeV) as a function of p (GeV), for $p_\nu < 2.4$GeV (left), and for a wider range of momenta (right).

plateau at about p=1.5 GeV, giving an estimate for Λ_{QCD} of about 300–600MeV in this renormalisation scheme.

4.5 Other form factors

A useful check on the symmetries of the vertex is to see whether form factors other than F_3 exhibit the behaviour expected of them according to (4.153). As a preliminary exercise, I have calculated $\mathrm{Tr}\Lambda_1(p, q = 0)$ for varying p_1 and p_4. At tree level, this is equal to $g_0 \sin p_1$, and in general it should be proportional to p_1 or $\sin p_1$. As figure 4.20 shows, this is indeed the case, at least qualitatively. It could also be argued that there is a constant term of ~ 0.02, and a slight linear dependence on p_t, but the uncertainties are so large that this cannot be ascertained with any confidence.

I have also computed $\mathrm{Tr}\gamma_5\Lambda_1$ and $\mathrm{Tr}\gamma_5\gamma_1\Lambda_1$, which should be zero because of parity conservation. This is confirmed.

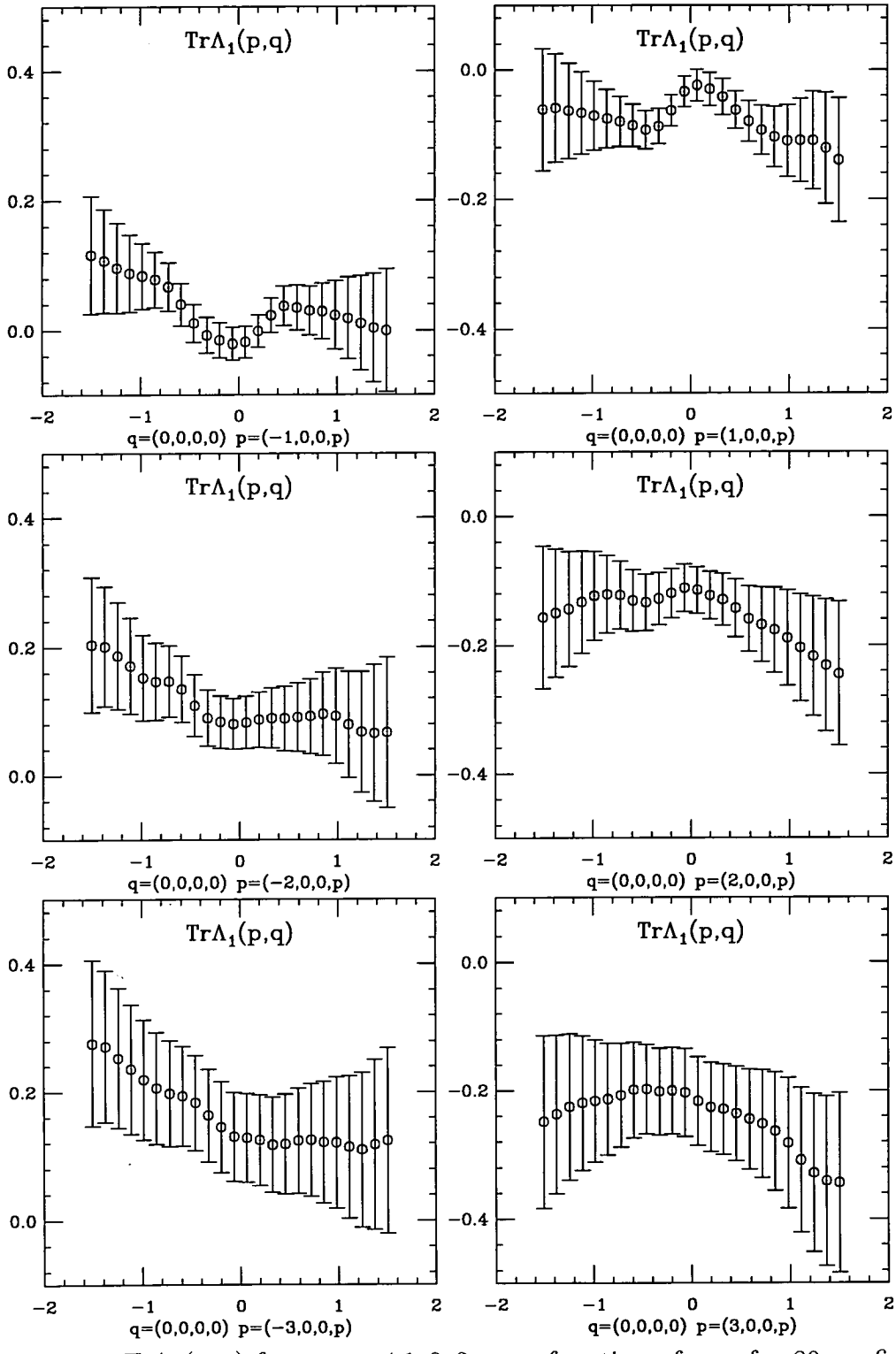

Figure 4.20: $\mathrm{Tr}\Lambda_1(p,q)$ for $n_{p_x} = \pm 1, 2, 3$, as a function of $p_t a$, for 80 configurations.

4.6 Outlook

4.6.1 Sources of error

As mentioned in section 4.3, off-shell Green functions will contain residual $\mathcal{O}(a)$ errors even when they are computed using the ($\mathcal{O}(a)$-improved) SW action. We have already seen that this gives uncertainties of 5% in the estimate for Z_2, from violations of rotational symmetry. Although no such violations are observed for the quark–gluon vertex, at least not for the kinematics used in this study, it is not unreasonable to assume that it also contains $\mathcal{O}(a)$ errors. Indeed this may be one reason why the signal deteriorates as rapidly with q as it does, to the extent that for $q_\nu a \geq 0.75$, with $p_\nu = 0$, all that can be observed is noise.

It is slightly puzzling that $\mathcal{O}(qa)$ errors are so large when $\mathcal{O}(pa)$ errors are relatively small. One explanation of this may be that the $\mathcal{O}(pa)$ effect is cancelled when amputating with $S(p)$ on both sides of the vertex, while $S(p+q)$ only enters once. This is supported by the plots (fig. 4.16) for $q_t \neq 0$, where the errors are smallest for $p + q/2 \approx 0$.

Considering the tree level expressions (1.51) and (4.164) for the quark propagator and the vertex function, it may be noted that the cosine term in the vertex will not contribute in the kinematics chosen for this study. The sine term in the quark propagator may on the other hand give $\mathcal{O}(a)$ contributions that are not taken care of by the amputation and the determination of Z_2.

Since the gluon is at zero momentum in the chosen kinematics, one would expect finite volume effects to play an important role. However, studies of the 3-gluon vertex [33] indicate that finite volume effects are not significant, even when zero-momentum gluons are involved. Still, it would be desirable to perform the simulation on a larger lattice in order to have a better resolution of the momentum in directions other than the time direction.

The gauge is fixed to an accuracy near machine precision. This should be an indication that errors due to inaccurate gauge fixing are small compared to other errors. I have not conducted any investigation of this kind of errors, but early studies of the quark propagator showed that gauge dependent quantities did not change significantly when the accuracy was changed from 10^{-6} to 10^{-11}.

Another potential source of uncertainties is Gribov copies. One would expect these to play some role, but studies of, among other things, gauge dependent determinations of current renormalisation constants [29] indicate that the errors due to Gribov copies are not large, and would not affect the qualitative results in this study.

The statistical errors are quite large, even with 332 configurations. This is not unexpected for gauge dependent, non-zero momentum 3-point functions. There seems to be little prospect of improving on the statistical errors at $\beta = 6.0$. Data taken at $\beta = 6.2$ would be expected to be less noisy, both because of self-averaging and because the Green functions are more well-defined at weak couplings.

A problem is that the perturbative window — where the effects of finite lattice spacing are small, and perturbation theory is still valid — is small. This means that comparisons with perturbation theory, or with lattice results obtained using different methods, is difficult. Simulations at higher β would reduce this problem as well.

4.6.2 Comparisons and applications

Matching these results for g_R to the $\overline{MS}$ scheme, and thereby to any other renormalisation scheme, is a fairly straightforward calculation in continuum perturbation theory. However, this has not yet been done, and no such calculations, using this specific scheme, are to my knowledge presented in literature. Without matching to other schemes, any comparison with other calculations or with experimental

results are fairly meaningless — although it is encouraging that the results for g_R are quite close to those of [33], where a similar renormalisation scheme was used.

This does not affect the main aim of this study, which has been to demonstrate the feasibility of the method, and despite the difficulties related to being restricted to a fermion action which is only on-shell improved, and the poor quality of the data for $q \neq 0$, this has been achieved.

Another potential application of this kind of study is to use the vertex as input in Dyson–Schwinger equations. The DSE for the quark self-energy $\Sigma(p) = \Sigma'(p) - \Sigma'(p = \mu)$ is

$$\Sigma'(p) = i\frac{4}{3}Z_\Lambda g^2 \int \frac{d^4q}{(2\pi)^4}\gamma_\mu S(q) D^{\mu\nu}(p-q)\Lambda_\nu(p,q) \qquad (4.172)$$

where $Z_\Lambda \Lambda_\mu(p,q)$ is the main unknown quantity. Usually, some ansatz is made about the form of it, after invoking the constraints of the Slavnov–Taylor identities. The remaining undetermined functions are determined using the DSE for the quark–gluon vertex — but that requires knowledge of the quark–quark scattering kernel, and only the asymptotic form of this is known. If the form of Λ_μ could be determined from the lattice, that would provide more solid input, or test the validity of the usual assumptions.

The methods employed in this study can easily be extended to the study of couplings between quarks and composite gluonic objects. Of particular phenomenological interest is the pomeron, which is assumed to be a 2-gluon $J^{PC} = J^{++}$ object (with J undetermined). Work is underway to investigate different models for this [35]. The methods are also similar to those involved in the non-perturbative renormalisation scheme discussed in section 2.3.2, which can be used to supplement the methods used in chapter 3. It is not surprising, however that the uncertainties in determinations of renormalisation constants using this method [18] are larger than those from the Ward identity and ratio methods discussed there.

4.6.3 Conclusions and suggestions for further work

The results presented in this chapter demonstrate that it is possible to extract the renormalised QCD running coupling non-perturbatively by studying the quark–gluon vertex on the lattice. Values for $\alpha_s(2\text{GeV})$ and Λ_{QCD} are found that are in reasonable agreement with results from other calculations and measurements. This is however only a qualitative result, since the perturbative matching to other schemes has yet to be done.

There is also a good prospect for computing the other form factors, thus determining non-perturbatively the complete (proper) quark–gluon vertex. A good signal for F_1 has already been found, and a more indepth study would attempt to quantify this and the remaining form factors. This would be useful especially for use in Dyson–Schwinger equations.

It is unsatisfactory that the gluon momentum has been fixed to zero when calculating physical quantities in this study. It would therefore be desirable to investigate the feasibility of using a renormalisation scheme where $p = -r = -q/2 = \mu$. There are indications that this might give useful results, especially from the data at $q_t \neq 0$, but other data, for q in other directions are not so encouraging.

The errors are still quite large, and apart from statistices, the most significant contribution is $\mathcal{O}(a)$ errors from the fermion action. It is clear that in order to obtain reliable results, it is important to bring these under control. Repeating these calculations with off-shell improved quark propagators would be a step in that direction. Reduction of the effects of finite lattice spacing would also be achieved by performing the calculations at higher β. This would have the added advantage of widening the perturbative window and (presumably) reducing statistical errors.

Although finite size effects are not expected to be large, it would be useful to quantify them by repeating the study on a lattice of different size.

Of more fundamental interest would be a study of the gauge dependence of the

vertex, including the effect of Gribov copies. Since any general covariant gauge, apart from the Landau gauge with Gribov copies, requires evaluation of multiple gauge transformations per configuration, this is considerably more expensive computationally, and is not a realistic prospect for the near future.

Conclusions

This thesis has studied the renormalisation of various quantities in lattice QCD. Renormalisation constants were computed non-perturbatively for the current renormalisation constants Z_A and Z_V, for the Sheikholeslami–Wohlert action. There is evidence that this would bring previous estimates for pseudoscalar and vector meson decay constants closer to their experimental values than the estimates obtained using the perturbative values, but there is still considerable discrepancy — at least for the UKQCD collaboration's results. Since this work was done over 2 years ago, more recent results have since appeared using more refined techniques and improved actions, for which the corresponding renormalisation constants to a large extent have yet to be computed.

A study was also conducted of the mass dependence of Z_V, using tadpole improved and non-improved actions, and different prescriptions for the $\mathcal{O}(a)$ improvement of the operators. This was little more than a study of the feasibility of the 'new' action and prescription, which had a positive outcome insofar as they are now both being used by the UKQCD collaboration.

In chapter 4, a method is presented for studying the quark–gluon vertex non-perturbatively and using it to extract a renormalised QCD coupling. The initial results of this are encouraging, although the perturbative matching to $\overline{MS}$ and other renormalisation schemes still has to be done in order to obtain physical predictions. The results are still hefted with large errors, especially $\mathcal{O}(a)$ errors from the quark field renormalisation constant, and this has to be brought under

control before more reliable estimates of the running coupling α_s and the scale parameter Λ_{QCD} can be obtained.

Bibliography

[1] K.G. Wilson, *Phys. Rev.* **D10**, 2445 (1974)

[2] H.B. Nielsen and M. Ninomiya, *Nucl. Phys.* **B185**, 20 (1981); *Nucl. Phys.* **B195**, 541 (1981); *Nucl. Phys.* **B193**, 173 (1981)

[3] K.G. Wilson, in A. Zichichi (ed.) *New Phenomena in Subnuclear Physics* Plenum Press, New York (1975)

[4] V.N. Gribov, *Nucl. Phys.* **B139**, 1 (1978)

[5] E. Marinari, C. Parrinello, R. Ricci, *Nucl. Phys.* **B362**, 487 (1991)

[6] L. Giusti, hep-lat/9605032

[7] D. Zwanziger, *Nucl. Phys.* **B345**, 461 (1990)
C. Parrinello and G. Jona-Lasinio, *Phys. Lett.* **B251**, 175 (1990)

[8] S. Fachin, C. Parrinello, *Phys. Rev.* **D44**, 2558 (1991)
D.S. Henty, O. Oliveira, C. Parrinello, S. Ryan, hep-lat/9607014

[9] H. Suman and K. Schilling, hep-lat/9512003

[10] K. Symanzik, *in* R. Schrader, R. Seiler and D.A. Uhlenbrock (eds), *Mathematical problems in theoretical physics*, Springer Lecture Notes in Physics, vol. 153 (1982)

[11] M. Lüscher, S. Sint, R. Sommer, P. Weisz, hep-lat/9605038.

[12] B. Sheikholeslami and R. Wohlert, *Nucl. Phys.* **B259**, 572 (1985)

[13] M. Lüscher et al, hep-lat/9608049, to be published in proceedings of Lattice 96.

[14] G.P. Lepage and P.B. Mackenzie, *Phys. Rev.* **D48**, 2250 (1993)

[15] T. Reisz, *Comm. Math. Phys.* **116**, 81, 573 (1988); *Comm. Math. Phys.* **117**, 79, 639 (1988); *Nucl. Phys.* **B318**, 417 (1989)

[16] M. Bochicchio et al., *Nucl. Phys.* **B262**, 331 (1985)

[17] G. Heatlie, G .Martinelli, C. Pittori, G.C. Rossi and C.T. Sachrajda, *Nucl. Phys.* **B352**, 266 (1991)

[18] G. Martinelli, C. Pittori, C.T. Sachrajda, M. Testa and A. Vladikas, *Nucl. Phys.* **B445**, 81 (1995)

[19] UKQCD collaboration (C.R. Allton et al.), *Nucl. Phys.* **B407**, 331 (1993)

[20] UKQCD collaboration (D.S. Henty), *Nucl. Phys.* **B (Proc. Suppl.) 34**, 468 (1994)

[21] G. Martinelli, S. Petrarca, C.T. Sachrajda and A. Vladikas, *Phys. Lett.* **B311**, 241 (1993)

[22] E. Gabrielli, G. Heatlie, G. Martinelli, C. Pittori and C.T. Sachrajda, *Nucl. Phys.* **B362**, 475 (1991)

[23] A. Borrelli, C. Pittori, R. Frezzotti and E. Gabrielli, *Nucl. Phys.* **B409**, 382 (1993)

[24] A. Vladikas, *Nucl. Phys.* **B(Proc.Suppl.)46**, 84 (1996)

[25] UKQCD collaboration (K.C. Bowler et al.), *Phys.Rev* **D52**, 5067 (1995)

[26] C.T. Sachrajda and N. Stella, in preparation.

[27] P.A. Rowland, to be published in proceedings of Lattice 96.

[28] A. Vladikas, C.T. Sachrajda, private communication.

[29] M.L. Paciello, S. Petrarca, B. Taglienti, A. Vladikas, *Phys. Lett.* **B341**, 187 (1994)

[30] UKQCD collaboration (C.R. Allton et al.), *Phys. Rev.* **D49**, 474 (1994)

[31] UKQCD Collaboration, in preparation; S.M. Ryan, Ph.D thesis (Edinburgh 1996).

[32] APE collaboration (C.R. Allton et al.) *Phys. Lett.* **B326**, 295 (1994)

[33] C. Parrinello, Phys. Rev. **D 50**, 4247 (1994); B. Allés, D. S. Henty, H. Panagopoulos, C. Parrinello, C. Pittori, hep-lat/960533

[34] C.T.H. Davies et al., *Phys. Rev.* **D37**, 1581 (1988)

[35] D. S. Henty, C. Parrinello, D. G. Richards, J. I. Skullerud, *Lattice Study of the Pomeron*, hep-ph/96072258, to be published in the Proceedings of Fourteenth Particles and Nuclei International Conference (PANIC96), Williamsburg, USA, May 1996.